

NASA Technical Memorandum 72862

CORRELATION OF PREDICTED AND MEASURED THERMAL STRESSES
ON AN ADVANCED AIRCRAFT STRUCTURE WITH SIMILAR MATERIALS

Jerald M. Jenkins

April 1979



NASA Technical Memorandum 72862

**CORRELATION OF PREDICTED AND MEASURED THERMAL STRESSES
ON AN ADVANCED AIRCRAFT STRUCTURE WITH SIMILAR MATERIALS**

Jerald M. Jenkins

**Dryden Flight Research Center
Edwards, California**



National Aeronautics and
Space Administration

1979

CORRELATION OF PREDICTED AND MEASURED THERMAL STRESSES
ON AN ADVANCED AIRCRAFT STRUCTURE WITH SIMILAR MATERIALS

Jerald M. Jenkins
Dryden Flight Research Center

INTRODUCTION

Several operational aircraft have accumulated significant flight time at speeds sufficient to produce severe aerodynamic heating (refs. 1 to 3). Even with this experience, there exists a lack of understanding of how accurately thermal stresses can be predicted on a complex structure. The ability to predict thermal stresses accurately has great impact on both the safe magnitude of stresses and the long-term effect of thermal cycling on the structure. An effort to study how well thermal stresses could be predicted in detail was begun in reference 4. This paper provides additional information about how laboratory measured thermal stresses compare with thermal stresses predicted using NASA structural analysis (NASTRAN) computer models and also with beam theory.

A test structure representing a portion of a hypersonic vehicle (ref. 5) was instrumented with strain gages and thermocouples. This test structure was then subjected to laboratory heating representative of hypersonic flight conditions. Several finite element computer models of this structure were developed using bar, shear panel, membrane, and plate elements of the NASTRAN program (ref. 6). A model derived from beam theory (ref. 7) was also developed. Temperature inputs from the tests were used to predict model thermal stresses, and these were correlated with the test measurements.

DESCRIPTION OF TEST SPECIMEN AND INSTRUMENTATION

A test specimen resulted from work directed toward studying the feasibility of a hypersonic research airplane (ref. 5). One structural concept resulting from this study was a heat sink type of structure. The basic philosophy was to use a variable-thickness, load-carrying skin to absorb heat as required to maintain a certain skin temperature. The skin was supported by a stainless steel zee substructure as shown in figure 1. A beryllium-aluminum composite metal (ref. 8) was selected as the skin because of the light weight and large thermal capacity of beryllium. The substructure frames were a zee-type configuration with type 301 stainless steel being used as the zee material. A photograph of the substructure frames is shown in figure 2. A photograph of the complete specimen is shown in figure 3 where the skins are attached to the substructure.

The location of the temperature and strain instrumentation is shown in figure 4. Sixteen thermocouples and sixteen strain gages were used for analysis purposes in this paper. Eleven thermocouples and strain gages were located on the skins, while the remaining five were located at strategic points on the substructure. Thermocouples and foil-type strain gages were used in the test temperature environment, which ranged from 241° K (-30° F) to 594° K (600° F).

TEST PROCEDURE

The general test setup is shown in the schematic in figure 5. The specimen is completely encased but is supported so that it is unrestrained--in other words, the edges are free to rotate and translate in the plane of the skin. A rack of radiant heaters (ref. 9) is located such that skins can be heated on the side away from the frames. A blower system is situated such that a mixture of air and gaseous nitrogen can be blown over the specimen if cooling is desired.

A flight profile for a hypersonic mission is shown in figure 6. This profile is of a 6-minute rocket-powered mission (ref. 5) with a 1-minute cruise at Mach 6. Skin temperatures were calculated based on the computer program identified in reference 10.

A time history of skin temperature of the profile was used to perform the test. The test specimen is cooled prior to heating to simulate the cold soak condition that occurs when rocket-powered aircraft are air launched at high altitude. After the

specimen is cooled, the heating is started by controlling the skin temperatures with radiant heaters according to the prescribed temperature time history.

DESCRIPTION OF THE STRUCTURAL MODELS

Beam Model

The concept of the beam thermal stress model is derived in reference 7 and the direct application is expanded in reference 11. One half of the test specimen was modeled symmetrically as shown in figure 7. The model, which has a surface area of .68 square meter (7.36 square feet) and a nominal depth of .10 meter (4 inches), was identified as BEAM and was composed of 29 elements. The effectiveness of a beam model must be tempered with the underlying assumptions discussed in the forementioned references. These assumptions include: sections remain perpendicular to the beam axis before and after loading, lateral contraction effects are neglected, and sections analyzed are remote from end effects.

NASTRAN Models

An initial NASTRAN model (shown in figure 8) was developed for one of the symmetrical quarters of the structure. This model, designated ASTEEL, was a 97 element model constructed of NASTRAN bar and shear panel elements. A second model, designated CSTEEL, was developed with a significantly changed grid arrangement. The CSTEEL model (shown in figure 9) contained 129 bar elements and 54 shear panel elements. There was little difference in thermal stress values between ASTEEL and CSTEEL models for consistent temperature cases. The CSTEEL model was selected as the basic NASTRAN model because the shear panel shapes were dimensionally more logical than for the ASTEEL model. It was decided to derive other models from the grid system of the basic CSTEEL model.

A model, designated DSTEEL, was developed with 129 bars, 36 shear panels, and 18 membrane elements. The shear panel elements in the skin of the CSTEEL model were replaced with membrane elements in the DSTEEL model. A model designated ESTEEL, was developed with 129 bars, 36 shear panels, and 18 plate elements. The shear panel elements in the skin of the CSTEEL model were replaced with plate elements in the ESTEEL model. A model, designated FSTEEL, was developed with 108 bars, 36 shear panels, and 18 plate elements. The longitudinal bars of the ESTEEL model were removed to result in the FSTEEL model. A Model, designated GSTEEL, was developed with 84 bars, 36 shear panels, and 18 plate elements. The lateral bars of the FSTEEL model were removed to

formulate the GSTEEL model.

A pictorial summary of all models used in this paper is shown in figure 10. A summary of the element type, grid points, degrees of freedom, single point constraints, and bulk data cards is presented in table 1. The grid point numbering system for the basic CSTEEL model is shown in figure 11.

RESULTS

The results of the hypersonic heating simulation will be examined in great detail for a single instant of time and in less detail on a time history basis. Temperatures for the hypersonic heating simulation begin near 241°K (-30°F) for the entire structure. Since previous hypersonic research aircraft are rocket powered, they are usually air launched from another aircraft to gain an altitude advantage. This very cold initial temperature soak represents the cold environment occurring at high altitude prior to air launching. The skins reach a maximum temperature near 594°K (600°F) while the substructure remains considerably cooler.

The structural temperature distribution for an instant in time (time = 4 minutes) is presented in figure 12. It is important to note that only the right spar and the skin areas between the panel centerlines are instrumented (see figure 4). The left spar and the adjacent skin to the left of the centerline are not instrumented. The temperature distribution for this area was assumed to be a mirror image of the adjacent spar and skin area. The temperature distribution presented in figure 12 was used as input information for the structural models described in the preceding section.

A comparison between thermal stresses measured during the laboratory heating tests and thermal stresses calculated using the structural models is presented in figure 13. The models, as a group, consistently agree with each other for both the spar thermal stresses and the skin thermal stresses. The measured thermal stresses in the spar area agree closely with the calculated thermal stresses. The major discrepancy exists in the web area closest to the skin. The calculated values are somewhat higher than the measured values. The calculated skin stresses are uniformly lower in magnitude than the measured values.

Since the data of figure 13 shows little variation between the calculations for the various structural models, the time histories of test data are presented with comparisons to only a single structural model. The CSTEEL model was selected as the primary comparison source for the computational aspects. Time histories of temperatures and laboratory measured thermal stresses are shown

in figure 14. Data for spar stresses are shown in figures 14(a) through 14(f). Data for skin stresses are presented in figures 14(g) through 14(k). The spar thermal stresses generally compare closely to calculated values. Location M, near the skin, appears to present the largest discrepancy in terms of percentage. Some minor discrepancies of up to 10 to 20 percent are seen at locations N and O. The correlation at P and Q is quite good. Some disagreement is seen at location R during the latter part of the flight profile.

Significant discrepancies are seen between the measured and calculated thermal stresses in the skin areas at locations A, C, and E (figures 14(g) through 14(i)). The correlation is good at locations G and I (figures 14(j) and 14(k)). It is important to note that the thermal stresses are not large numbers in the skin areas. It is interesting to note the apparent strain curve, which is presented in figure 15. The thermal expansion properties of Be-38Al and 301 stainless steel are identical; hence the same apparent strain curve can be used for both materials.

DISCUSSION

The primary purpose of this paper is to evaluate how well thermal stress can be predicted using finite element models. A beam theory model was developed and several NASTRAN models were also developed. The family of structural models used for analysis was presented in figure 10.

It was shown in figure 13 that there was quite close agreement among the various models. There was, however, significant discrepancy between the measured thermal stresses and the predicted thermal stresses. The basic NASTRAN model was constructed of shear panel and bar elements. In order to study the impact of using different combinations of elements, bar, membrane, and plate elements were introduced as representations of the skin. These changes in the elements resulted in very little change in the calculated answers.

It is important to focus on the apparent discrepancies between the predicted and measured thermal stresses. Since the beam model and all the NASTRAN models result in very similar answers (figure 13), it is logical to assume that the reason for the discrepancy does not lie with the model source. Several potential sources for the discrepancy were investigated; however, the most logical problem area that was revealed involved the adequacy of the temperature input with respect to the size of the model.

A heating test was conducted in reference 4 that was identical

in nature to the experiment of this paper. The skin of both specimens was subdivided as shown in figure 16 so that the skin temperature in each zone was controlled with a thermocouple feed-back heating arrangement, as previously described in the TEST PROCEDURE section. The temperature at the center of each of the nine skin panels is shown in figure 16. It can be seen that the temperature variation of the skin panels of reference 4 is very small. The skin temperatures were controlled very uniformly with no gradients in the plane of the skins.

A comparable temperature distribution for the experiment conducted in this paper is shown in figure 16(b). It can easily be seen that the three shaded panels experience temperatures distinctly different from the other six panels. This anomaly was noted at the time of the test; however, it was thought that the effect would be negligible. The variation is greatest between the center panel, where the temperature is too high, 600°K (610°F), and the upper right panel, which has a low temperature of 561°K (542°F). This variation may have greater impact than was first thought.

The test panel in this paper was not as well instrumented as the test panel in reference 4. The temperature instrumentation extended from the middle of the center panel to the middle of the left panel (see figure 4). The NASTRAN models were represented as one quarter of the test specimen and the beam model was represented as one half of the test specimen (see figures 7 and 8 respectively). Only one eighth of the cross section was instrumented with thermocouples. There was no temperature information for input for the outer spar (figure 12) or the skin near the outer spar. The distributions in these areas were considered to be mirror images of the adjacent skin and spar. It was also assumed that the temperature did not vary in the Y-direction.

It is difficult, after the fact and without additional testing, to pinpoint an exact cause of a discrepancy such as is seen in figure 13. One thing that was apparent in figure 16 is that the temperature input to the outer spar and skin were most likely lower than was assumed.

An effort to study this is presented in figures 17 and 18. The circular symbols of figure 17 represent the assumed temperature distribution used for the NASTRAN models (CSTEEL was used to study this particular anomaly). The square and diamond symbols represent 28°K (50°F) and 56°K (100°F) lower temperature perturbations, respectively, in the area where the temperatures were thought to be assumed too large. These perturbed temperatures were input to the CSTEEL NASTRAN model and the comparison with the original thermal stress values is presented in figure 18. Both of these perturbations changed the thermal stress values (closest to the

area where the temperature was perturbed) such that closer agreement with the measured thermal stress values occurred. This strongly suggests that inadequate temperature input data was available for input to the structural model. The amount of input data was inadequate because the uniformity of the heating of the test specimen was not sufficiently controlled to be compatible with the assumptions used for the structural models. This is a major result since there is little established at this time concerning the detail with which temperatures must be supplied to structural models to achieve good thermal stress calculations. The results of this paper indicate a high degree of structural model sensitivity to errors or inadequacies in temperature information.

CONCLUDING REMARKS

There are two very important objectives addressed in this paper. The first is to enhance the general knowledge of applying finite element structural models to thermal stress problems. The second is to begin to establish a data base from which estimates of required model complexities can be obtained with respect to temperature input requirements, resulting thermal stresses, and the type of structural elements required.

Six NASTRAN models and a beam model were used to develop calculated thermal stresses. The six NASTRAN models utilized various combinations of bar, shear panel, membrane, and plate elements. It was found that for a given temperature distribution there was very little variation in calculated thermal stresses when element types were interchanged for a given grid system. The resulting thermal stresses calculated for the beam model compared similarly to the values obtained for the NASTRAN models. All of the structural models considered in this paper resulted in calculating essentially the same values of thermal stresses for a given temperature-environment.

A discrepancy of significance occurred between the measured and predicted thermal stresses in the skin areas. A minor anomaly in the uniformity of the specimen skin temperatures is thought to have been the cause of this discrepancy. The anomaly in the skin heating uniformity resulted in inadequate temperature input data for the structural model. Perturbations of the skin temperature distributions and recalculations of the thermal stresses substantiated this hypothesis. The results of this paper indicate a high degree of structural model sensitivity to errors or inadequacies in the temperature information.

Dryden Flight Research Center
National Aeronautics and Space Administration
Edwards, Calif., February 20, 1979

REFERENCES

1. Quinn, Robert D.; and Olinger, Frank V. (appendix A by James C. Dunavant and Robert L. Stallings, Jr.): Heat-Transfer Measurements Obtained on the X-15 Airplane Including Correlations With Wind-Tunnel Results. NASA TM X-1705, 1969.
2. Andrews, William H.: Summary of Preliminary Data Derived From The XB-70 Airplanes. NASA TM X-1240, 1966.
3. Quinn, Robert D.; and Olinger, Frank V.: Flight Temperatures and Thermal Simulation Requirements. NASA YF-12 Flight Loads Program, NASA TM X-3061, 1974, pp. 145-183.
4. Jenkins, Jerald M.; Schuster, Lawrence S.; and Carter, Alan L.: Correlation of Predicted and Measured Thermal Stresses on a Truss-Type Aircraft Structure. NASA TM-72857, November, 1978.
5. Combs, H. G., et al.: Configuration Development Study of the X-24C Hypersonic Research Airplane - Executive Summary. NASA CR 14274, 1977.
6. McCormick, Caleb W., ed.: The NASTRAN User's Manual (Level 15). NASA SP-222(01), 1972.
7. Boley, Bruno A.; and Weiner, Jerome H.: Theory of Thermal Stresses. New York. John Wiley & Sons, Inc., 1962.
8. Aerospace Structural Metals Handbook. Volume 4 - Non-Ferrous Alloys. AFML-TR-68-115, Air Force Materials Lab., Wright-Patterson AFB, 1978.
9. Sefic, Walter J.; and Anderson, Karl F.: NASA High Temperature Loads Calibration Laboratory. NASA TM X-1868, 1969.
10. Gord, P. R.: Measured and Calculated Structural Temperature Data From Two X-15 Airplane Flights With Extreme Aerodynamic Heating Conditions. NASA TM X-1358, 1967.
11. Jenkins, Jerald M.: A Pretensioning Concept for Relief of Critical Leading-Edge Thermal Stress, NASA TN D-3507, July, 1966.

TABLE 1. SUMMARY OF STRUCTURAL MODEL CHARACTERISTICS.

Model	Element				Grid Points	Degrees of Freedom	Single Point Constraints	Bulk Data Cards
	Bar	Shear Panel	Membrane	Plate				
ASTEEL	73	24	0	0	50	231	69	250
CSTEEL	129	54	0	0	76	387	69	402
DSTEEL	129	36	18	0	76	375	81	402
ESTEEL	129	36	0	18	76	375	81	402
FSTEEL	108	36	0	18	76	375	81	376
GSTEEL	84	36	0	18	76	375	81	349
BEAM	29							

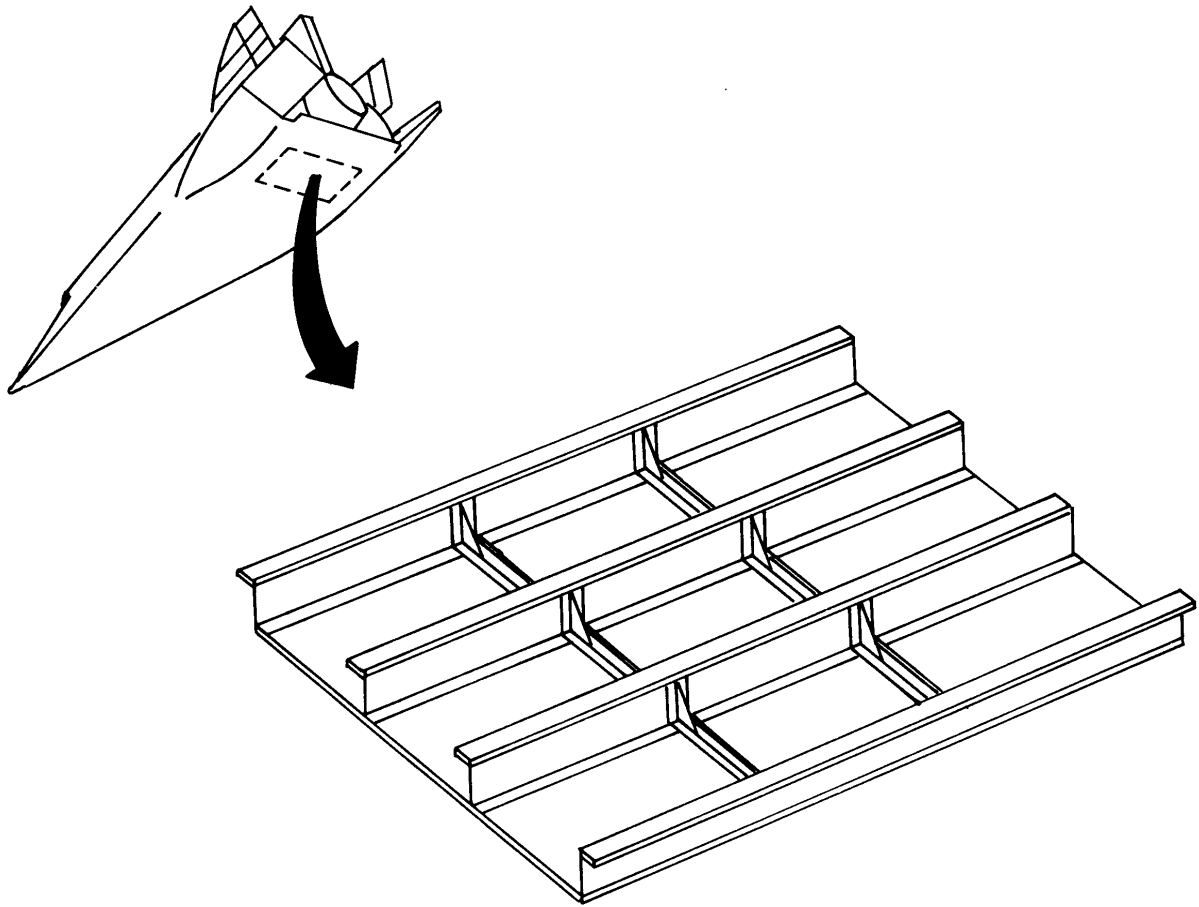


Figure 1. Location of test specimen on hypothetical hypersonic airplane.

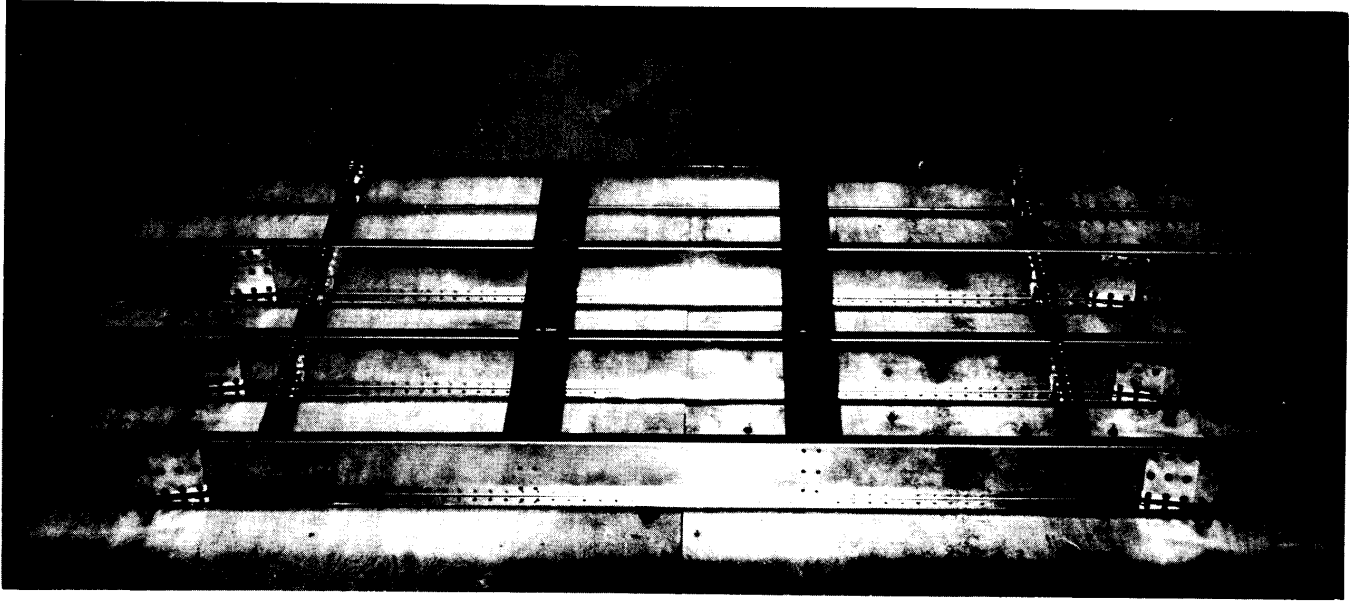
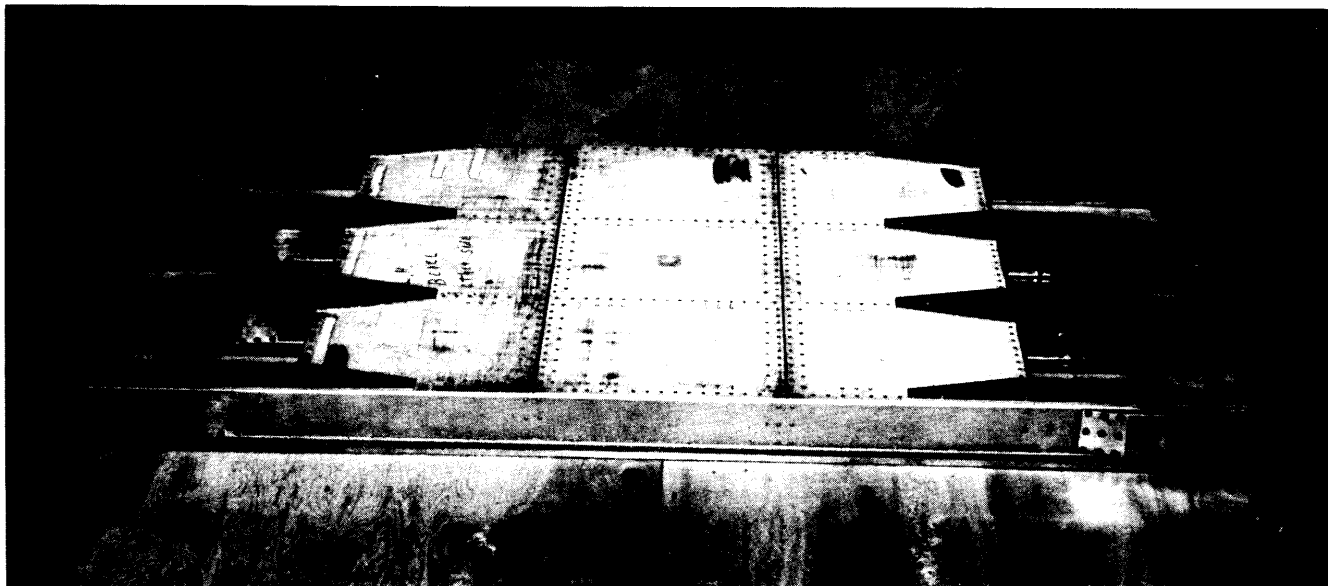


Figure 2. Stainless steel zee substructure frames.

E-31363



E-31364

Figure 3. Stainless steel zee/beryllium-aluminum skin test component.

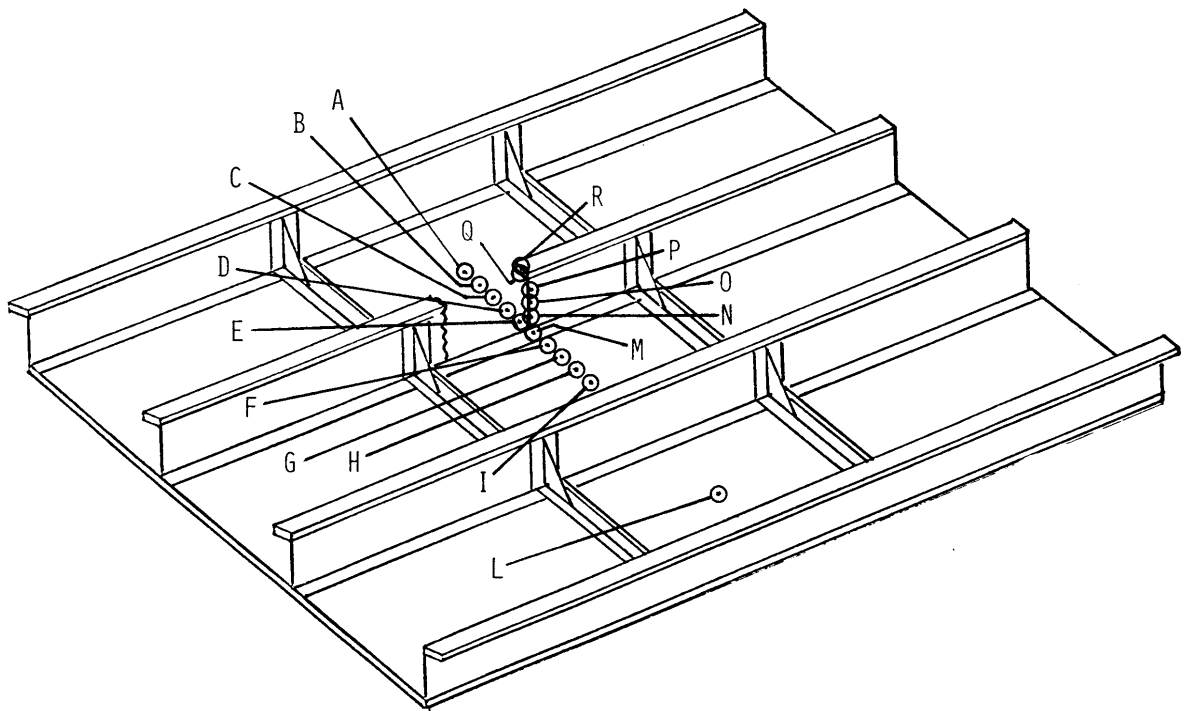


Figure 4. Location of strain gages and thermocouples used for analysis.

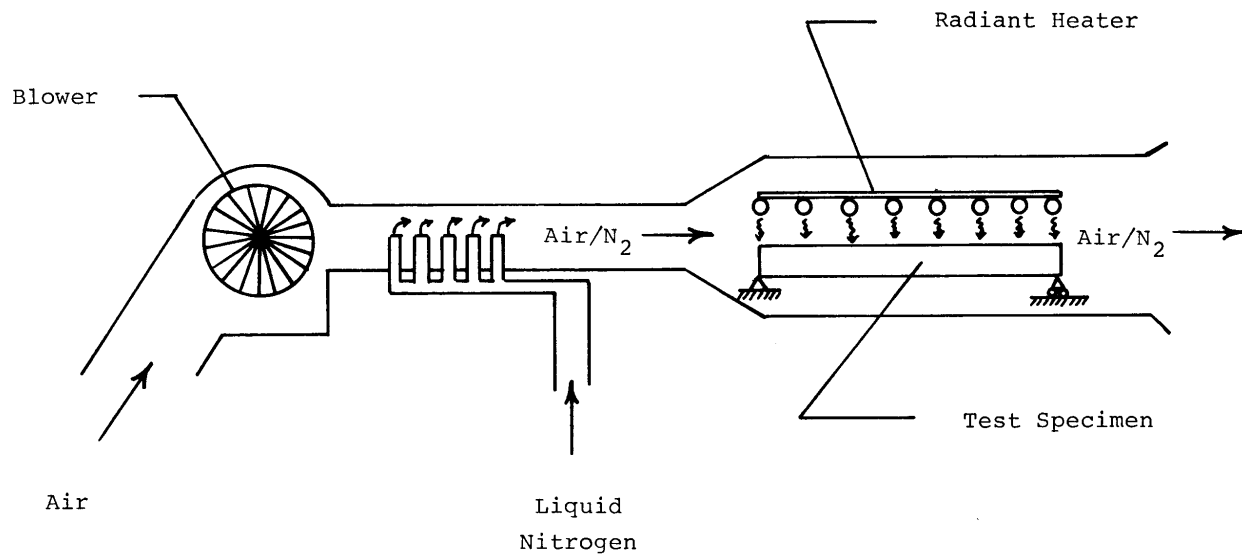


Figure 5. Schematic illustrating the general test setup.

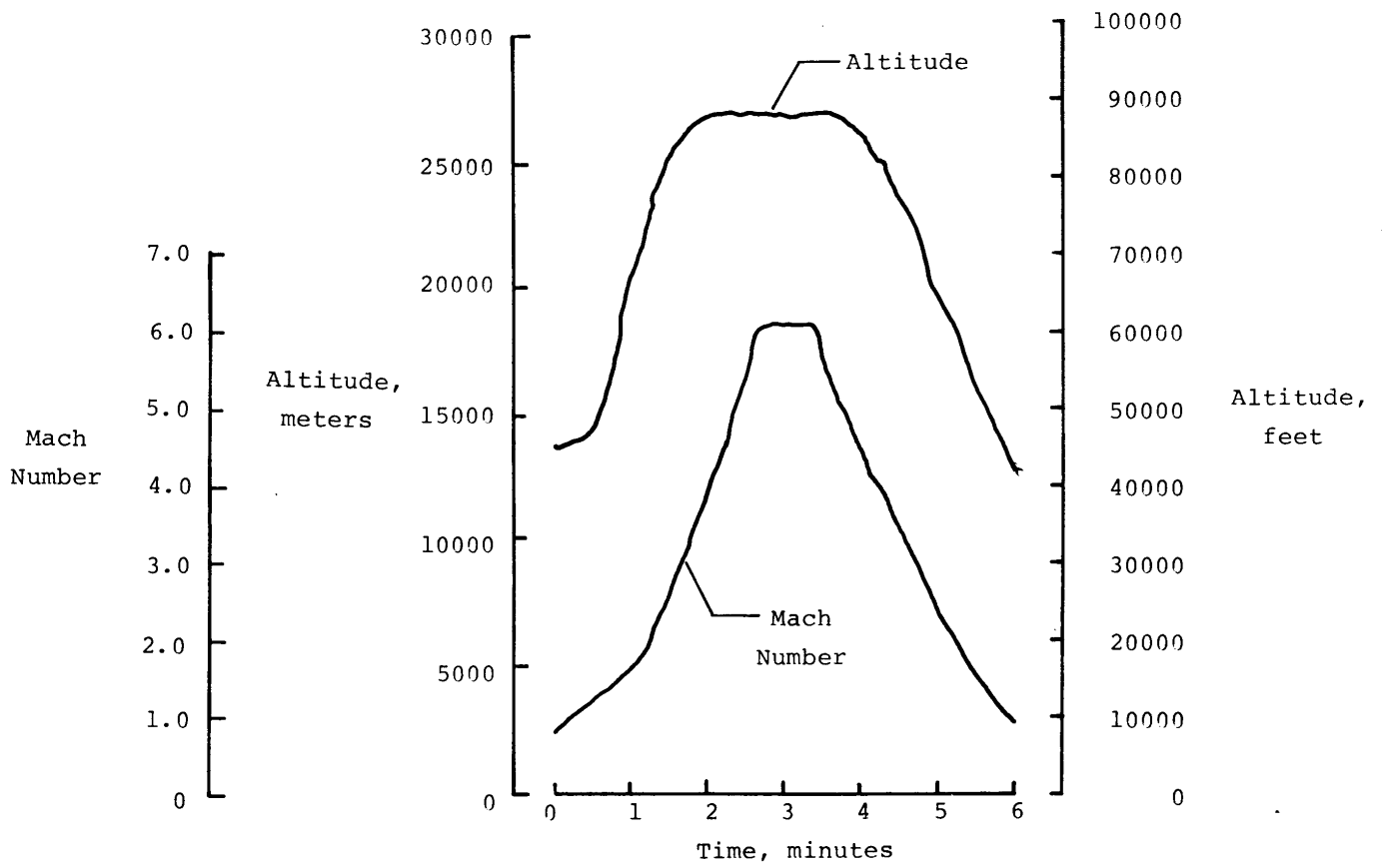


Figure 6. Time history of altitude and Mach number for a hypersonic flight.

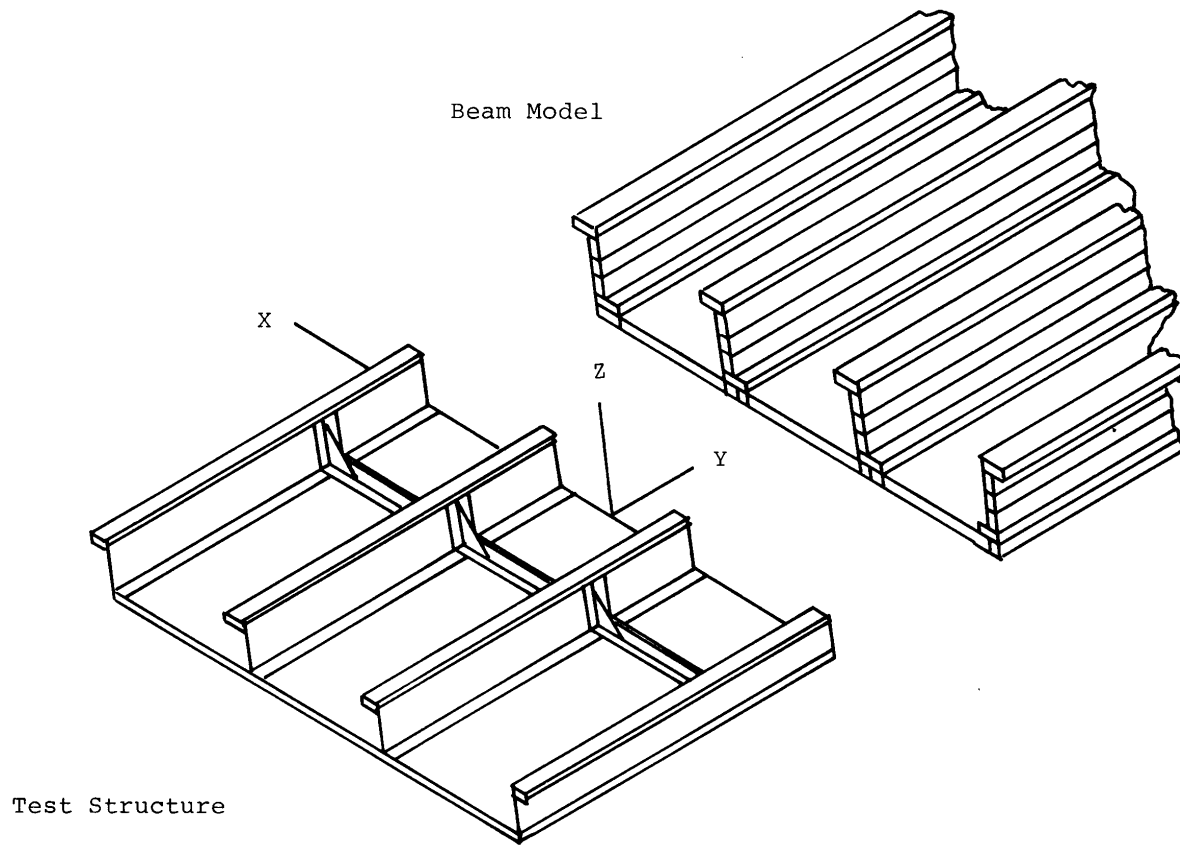


Figure 7. Test structure showing location of structural model.

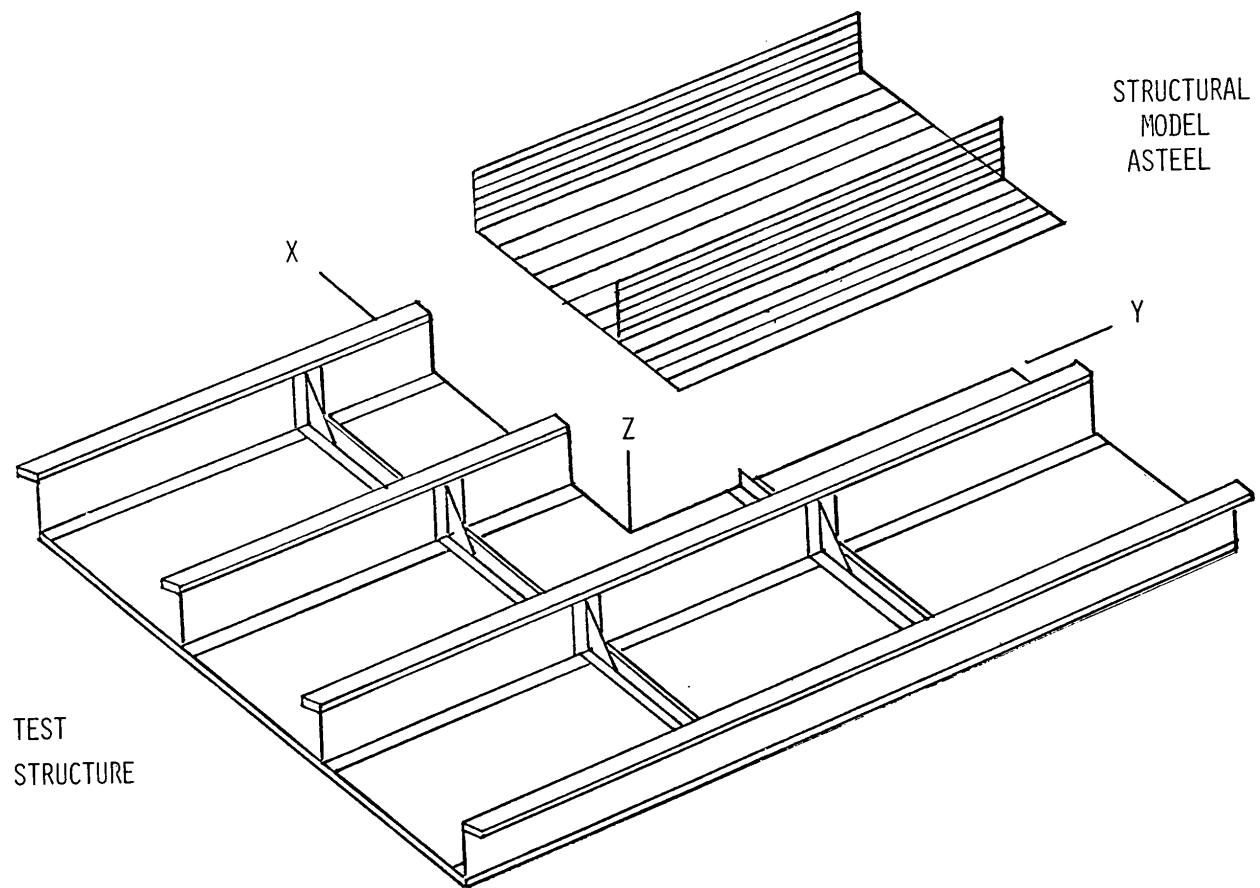


Figure 8. Test structure showing location of structural model.

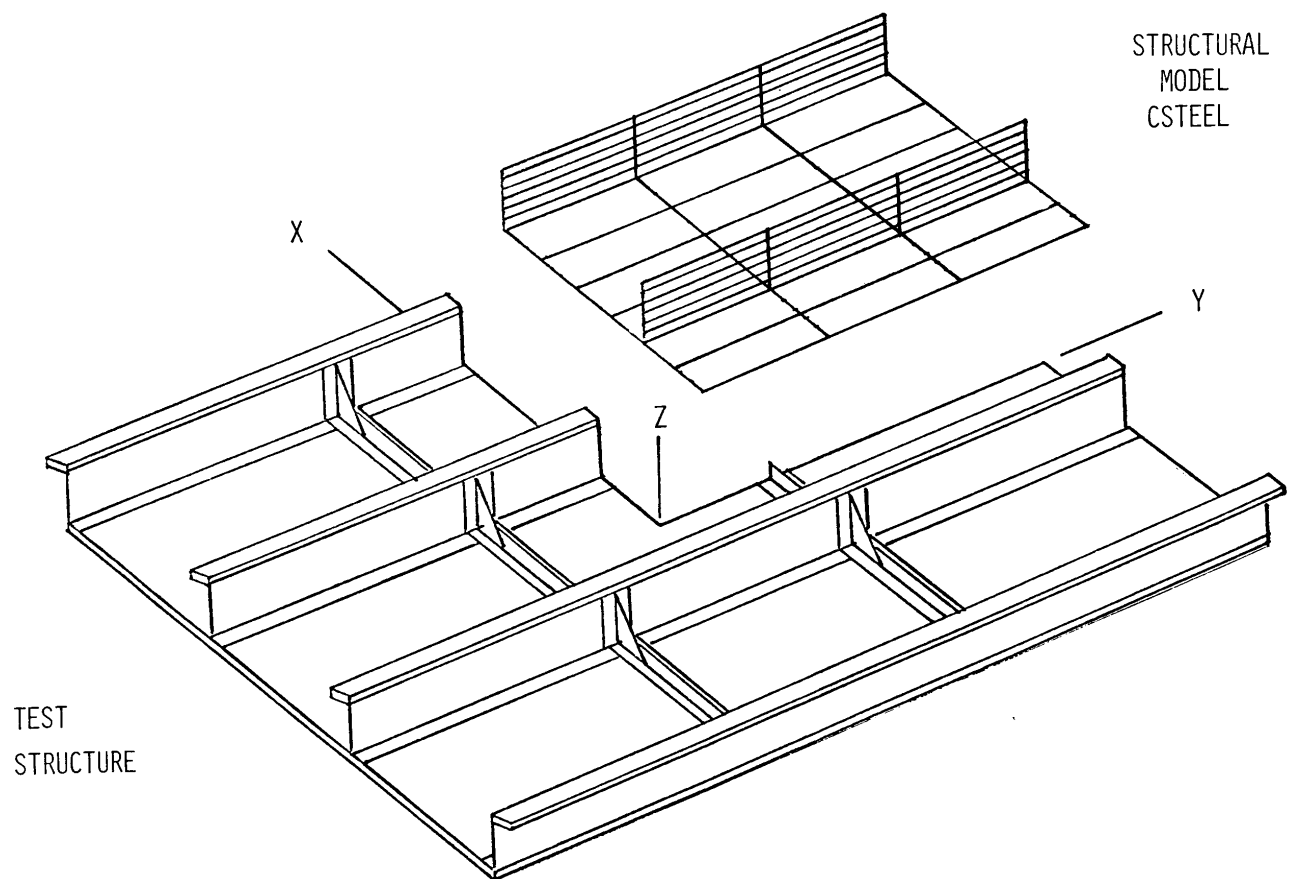


Figure 9. Test structure showing location of structural model.

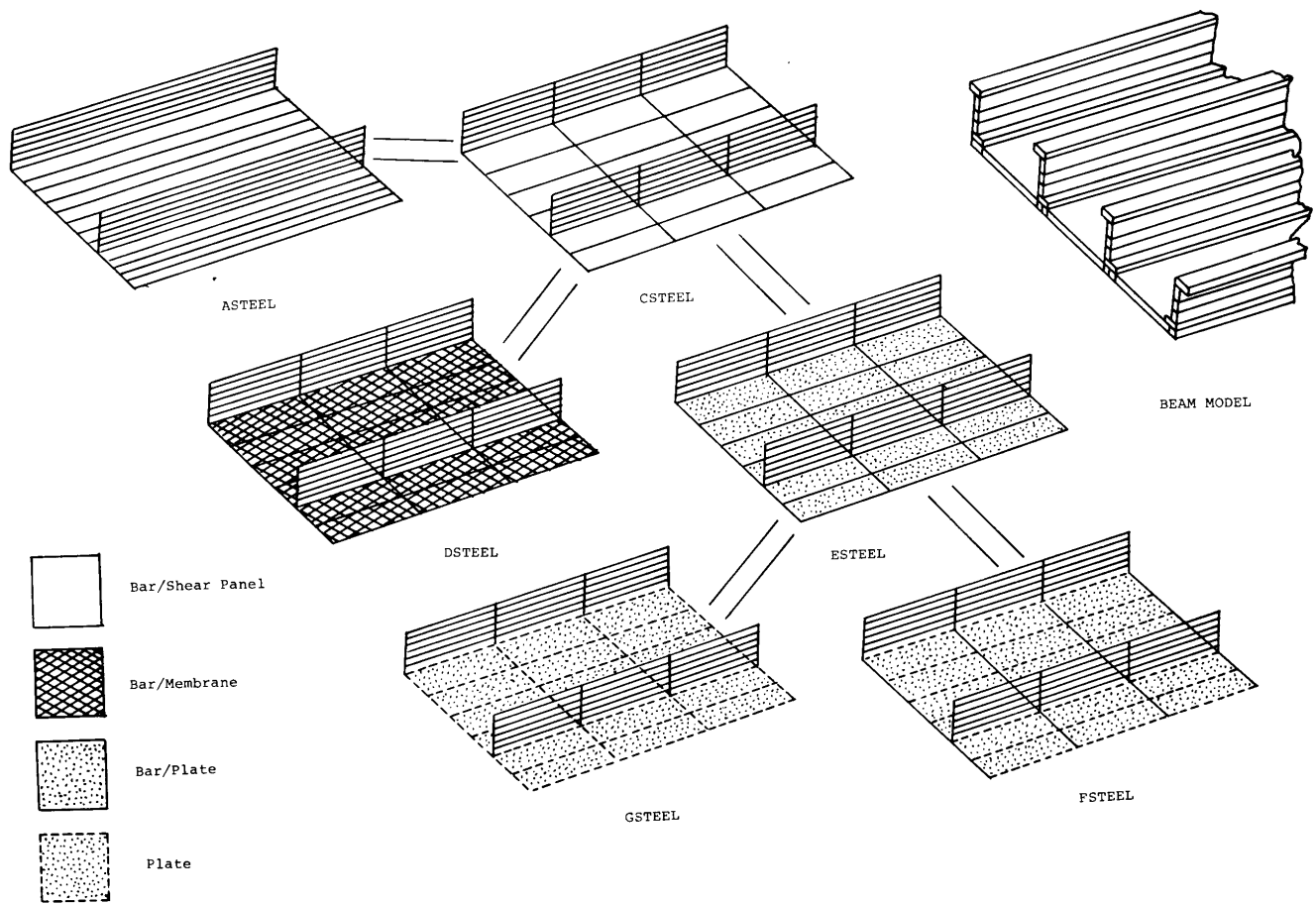


Figure 10. Family of structural models used for analysis.

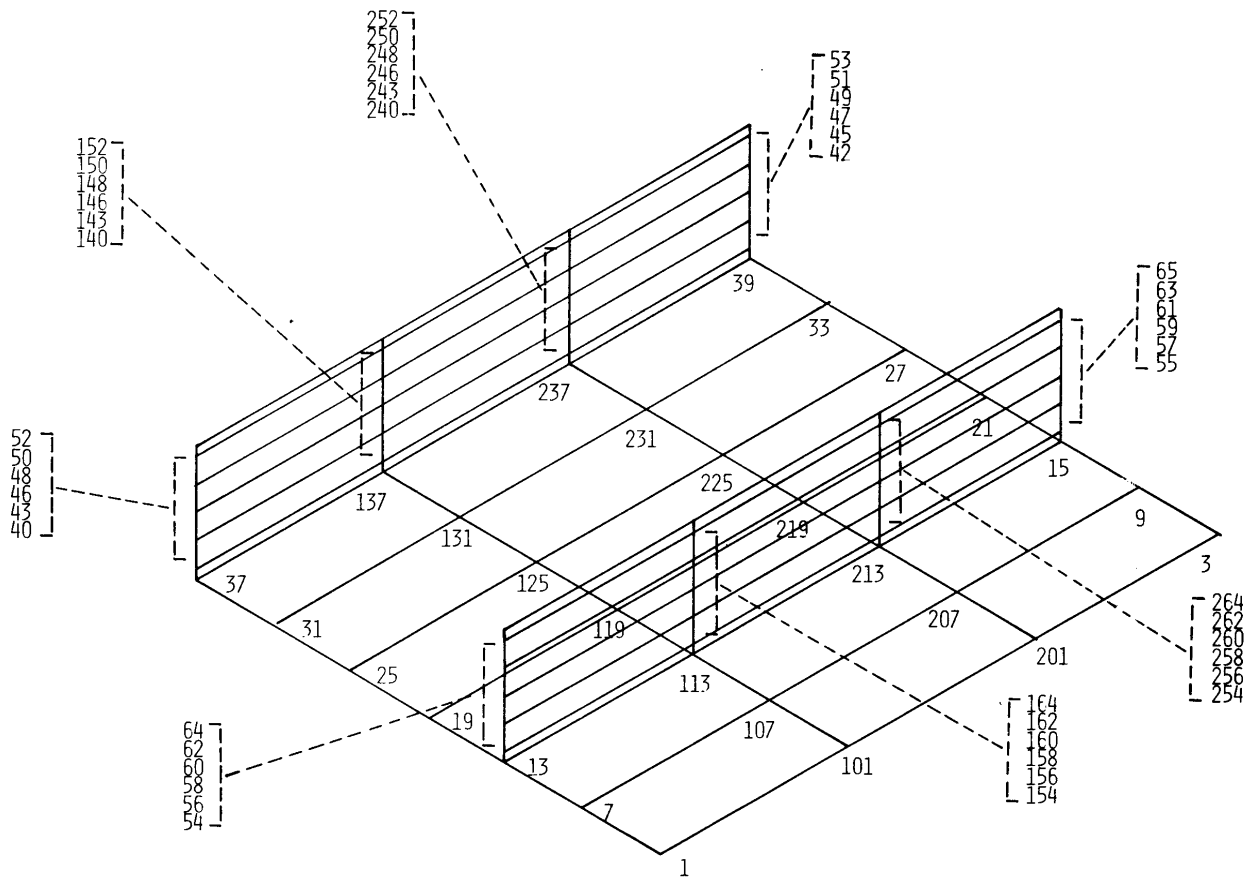


Figure 11. Grid point numbering system for NASTRAN model.

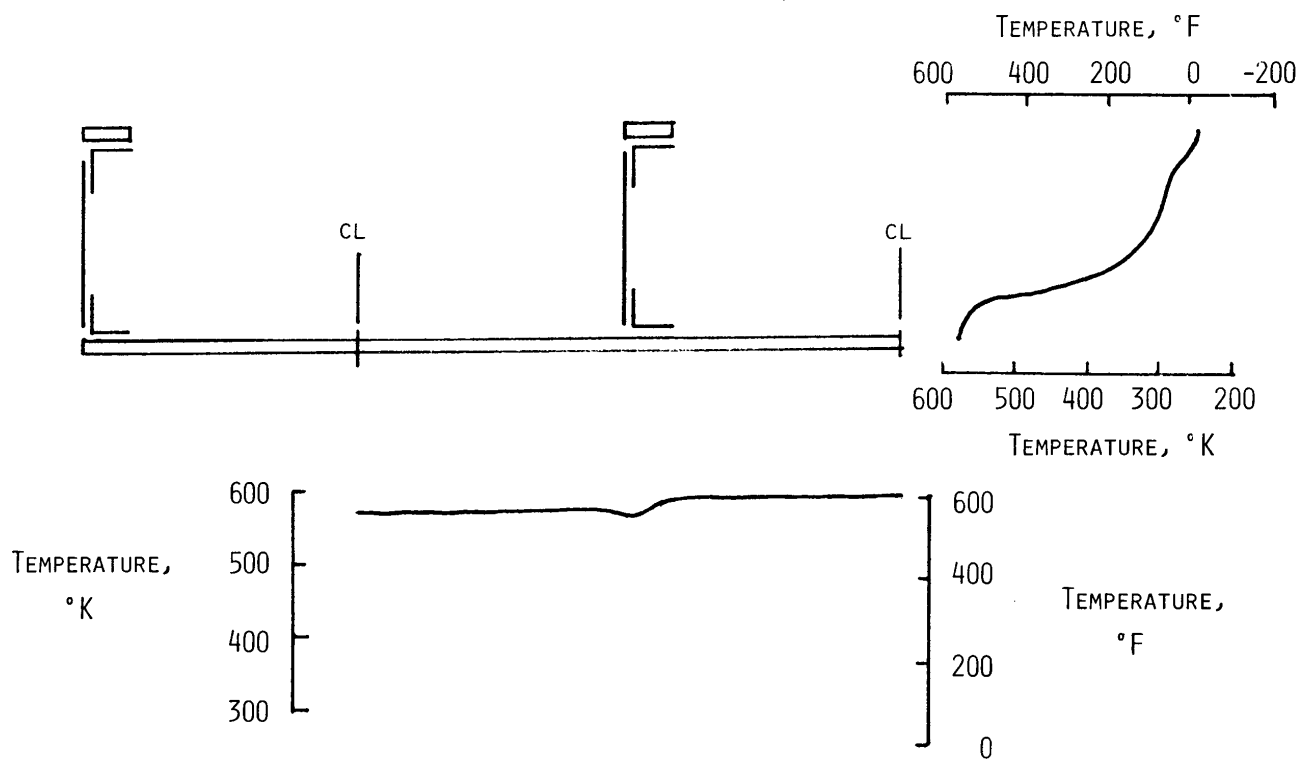


Figure 12. Distribution of measured temperatures for the hypersonic profile. Time = 4 minutes.

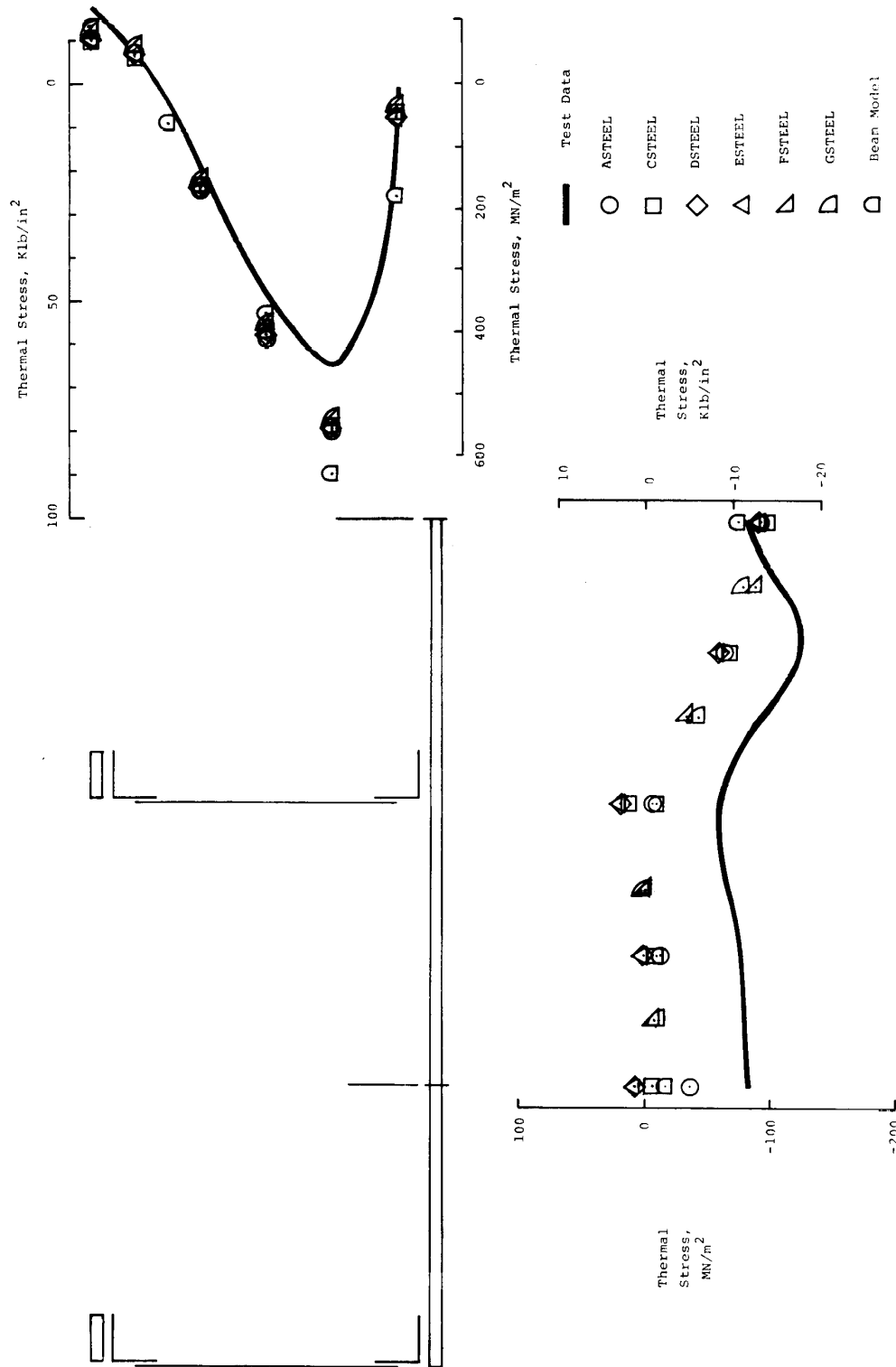
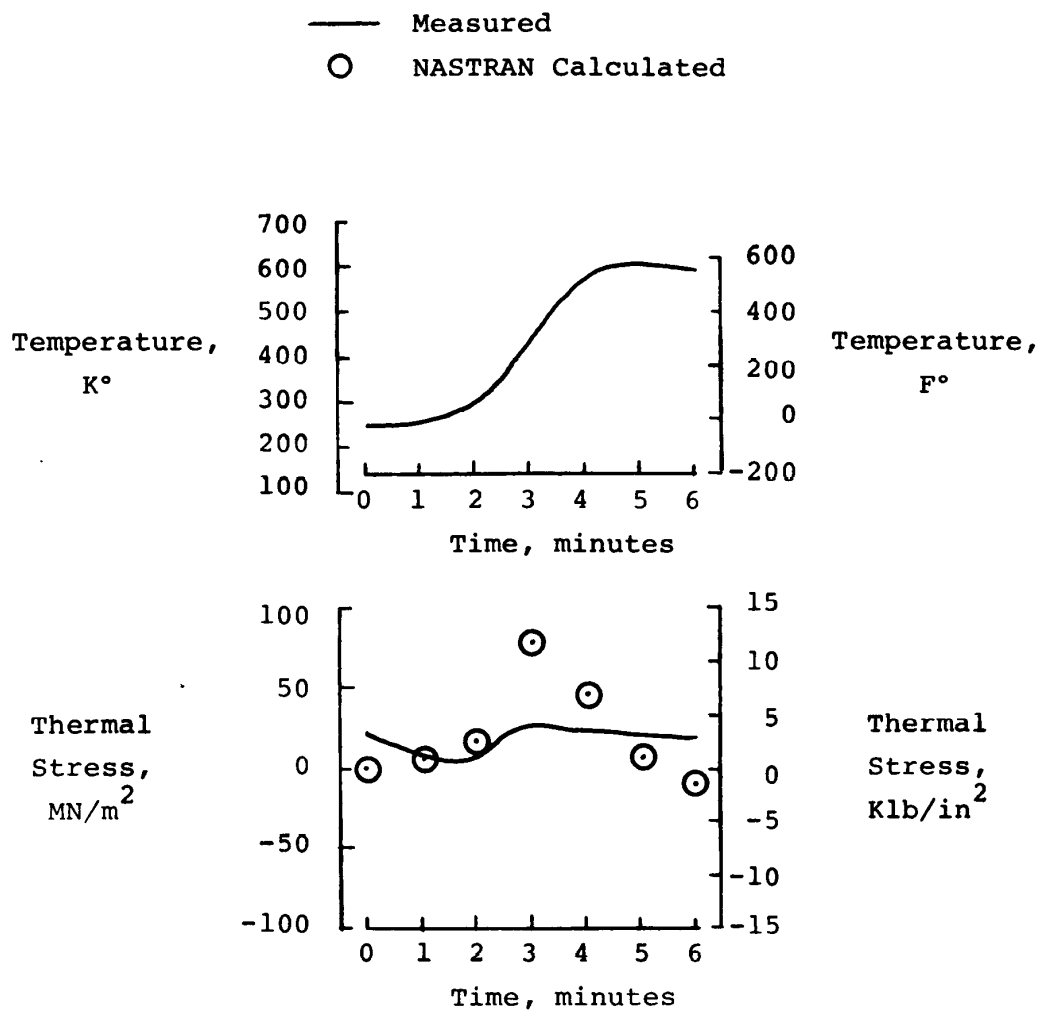
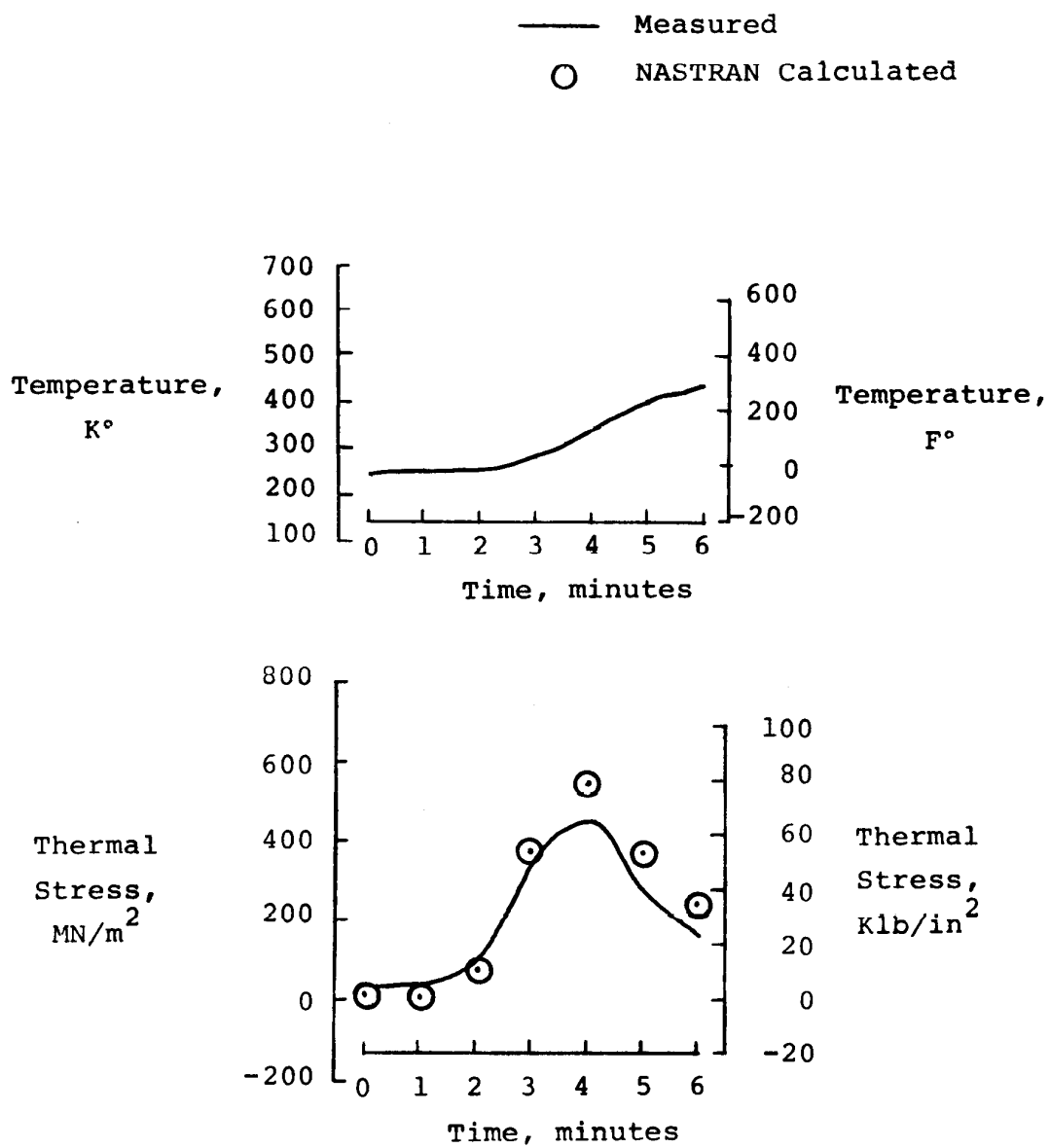


Figure 13. Comparison of measured and NASTRAN-calculated thermal stress distribution for the hypersonic profile. Time = 4 minutes.



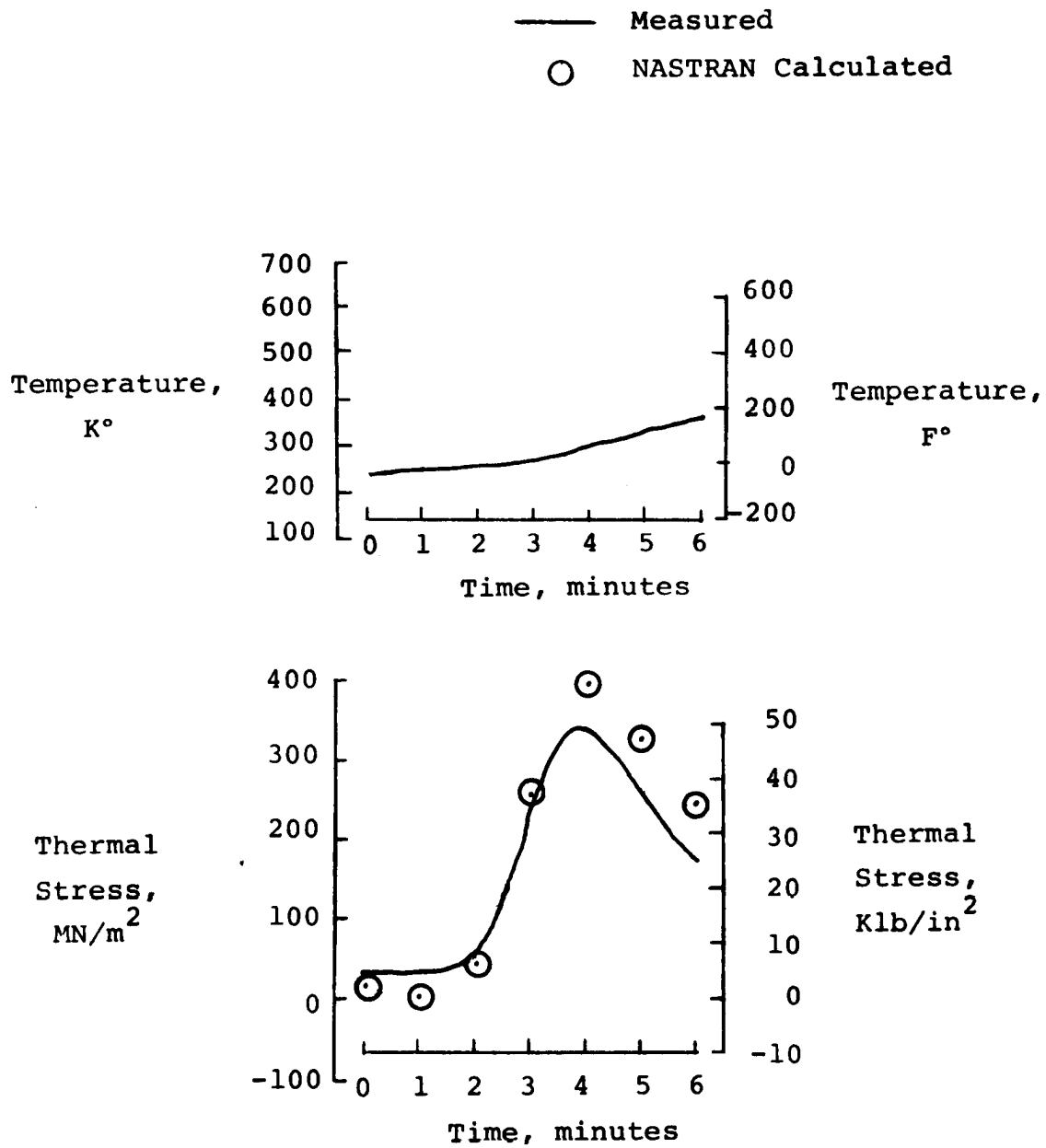
(a) Location M.

Figure 14. Measured temperatures and comparison of measured and NASTRAN-calculated thermal stresses for hypersonic heating simulation.



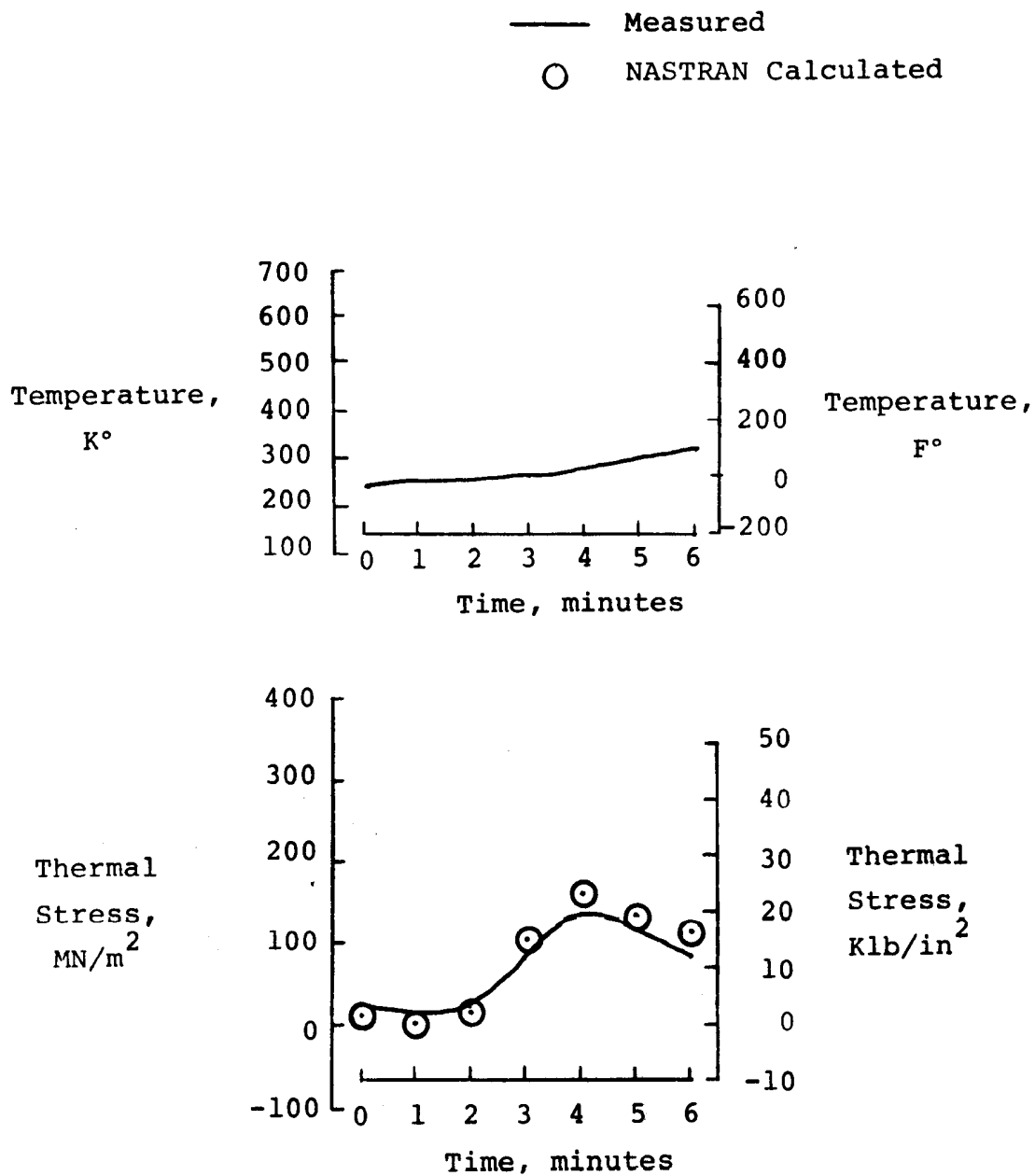
(b) Location N.

Figure 14. Continued.



(c) Location O.

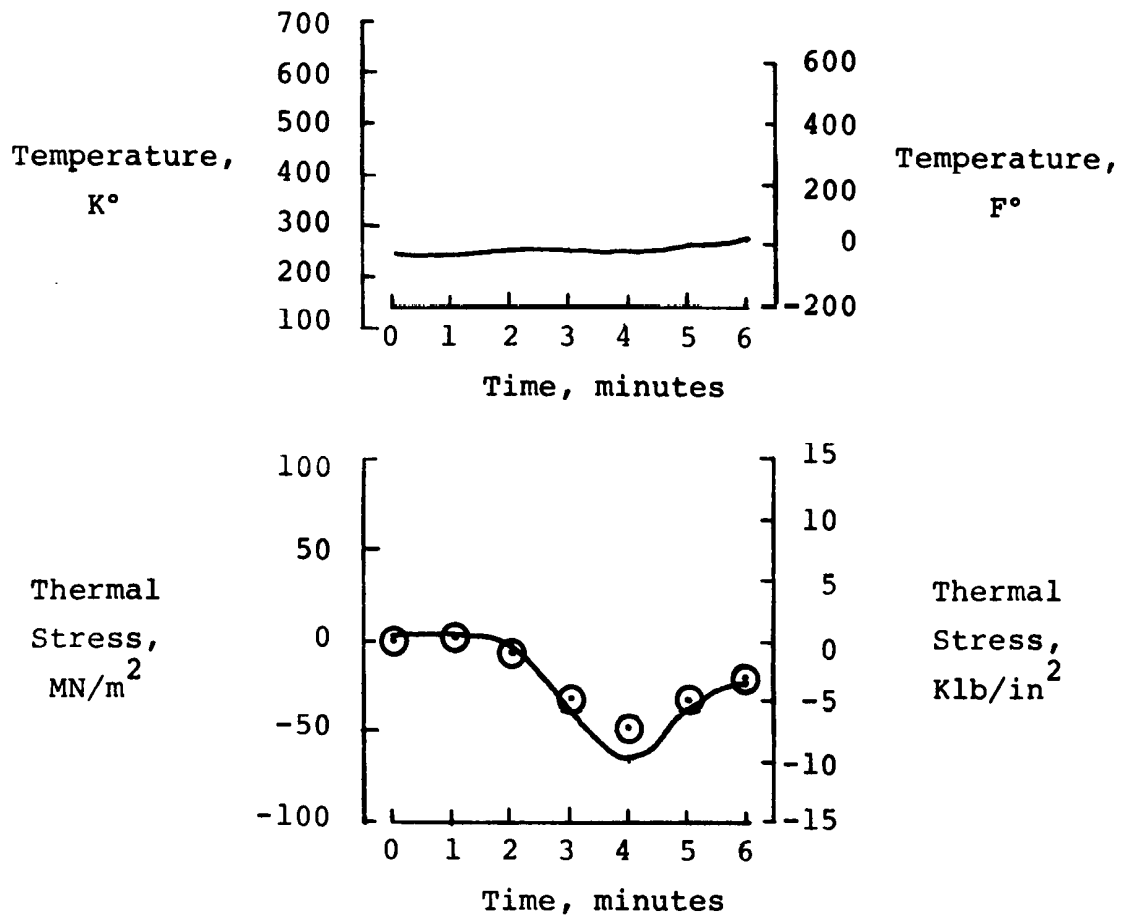
Figure 14. Continued.



(d) Location P.

Figure 14. Continued.

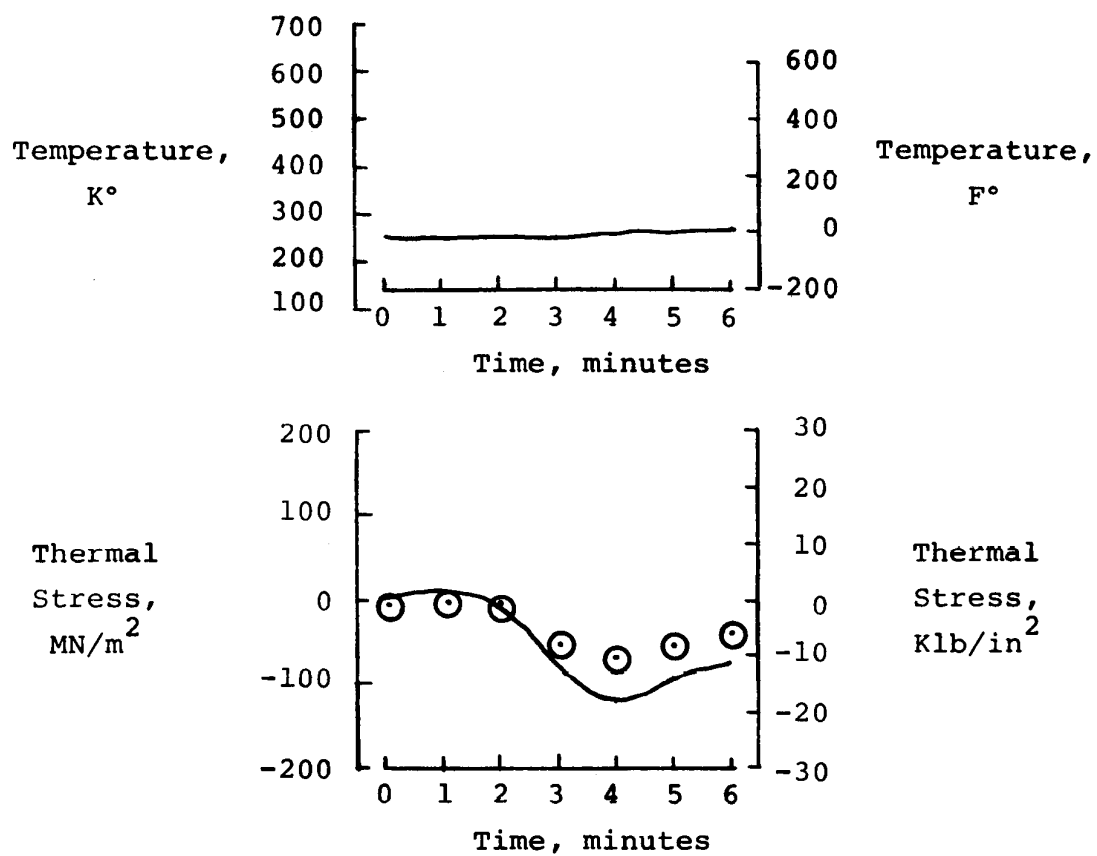
— Measured
○ NASTRAN Calculated



(e) Location Q.

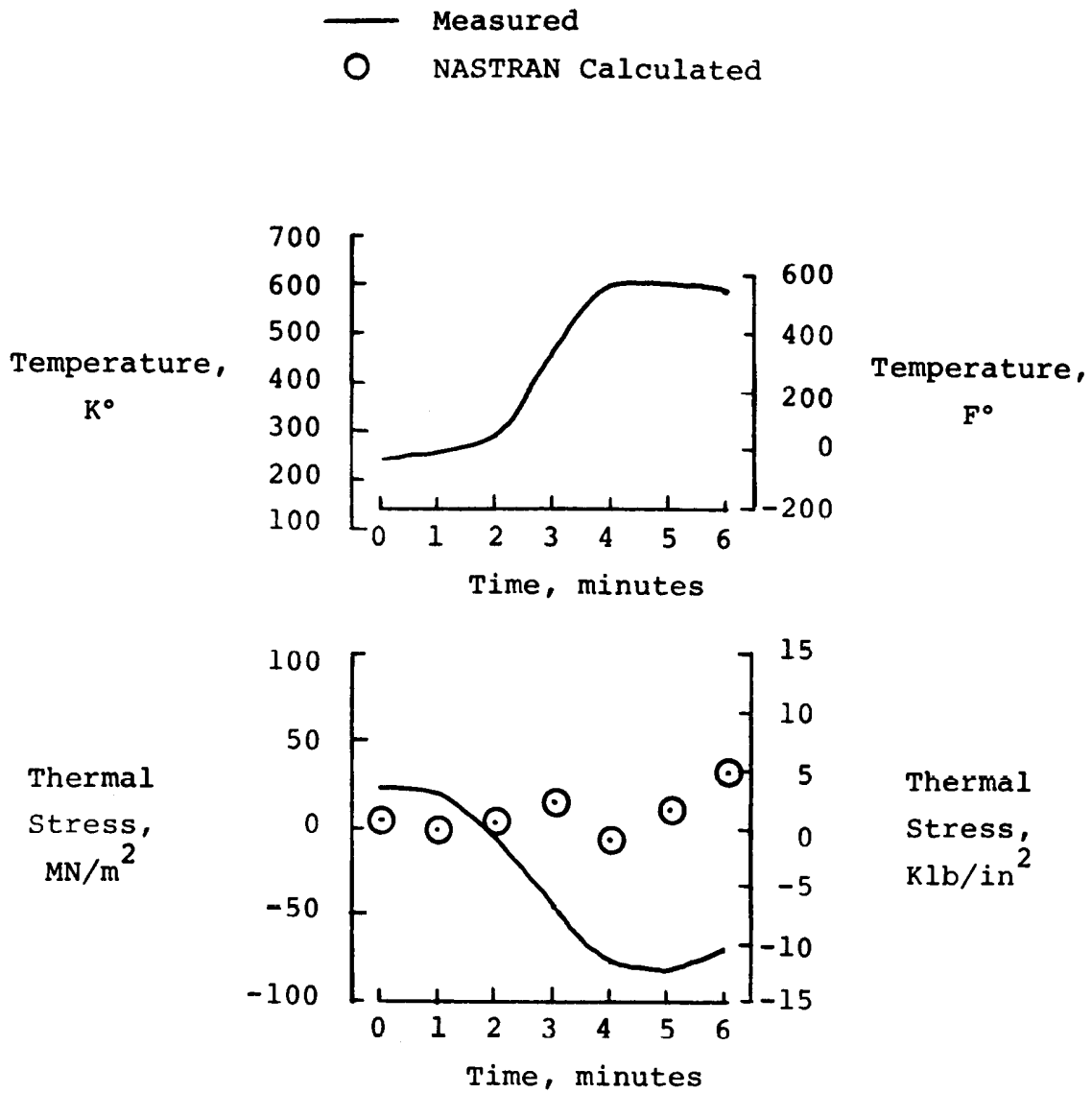
Figure 14. Continued.

— Measured
 ○ NASTRAN Calculated



(f) Location R.

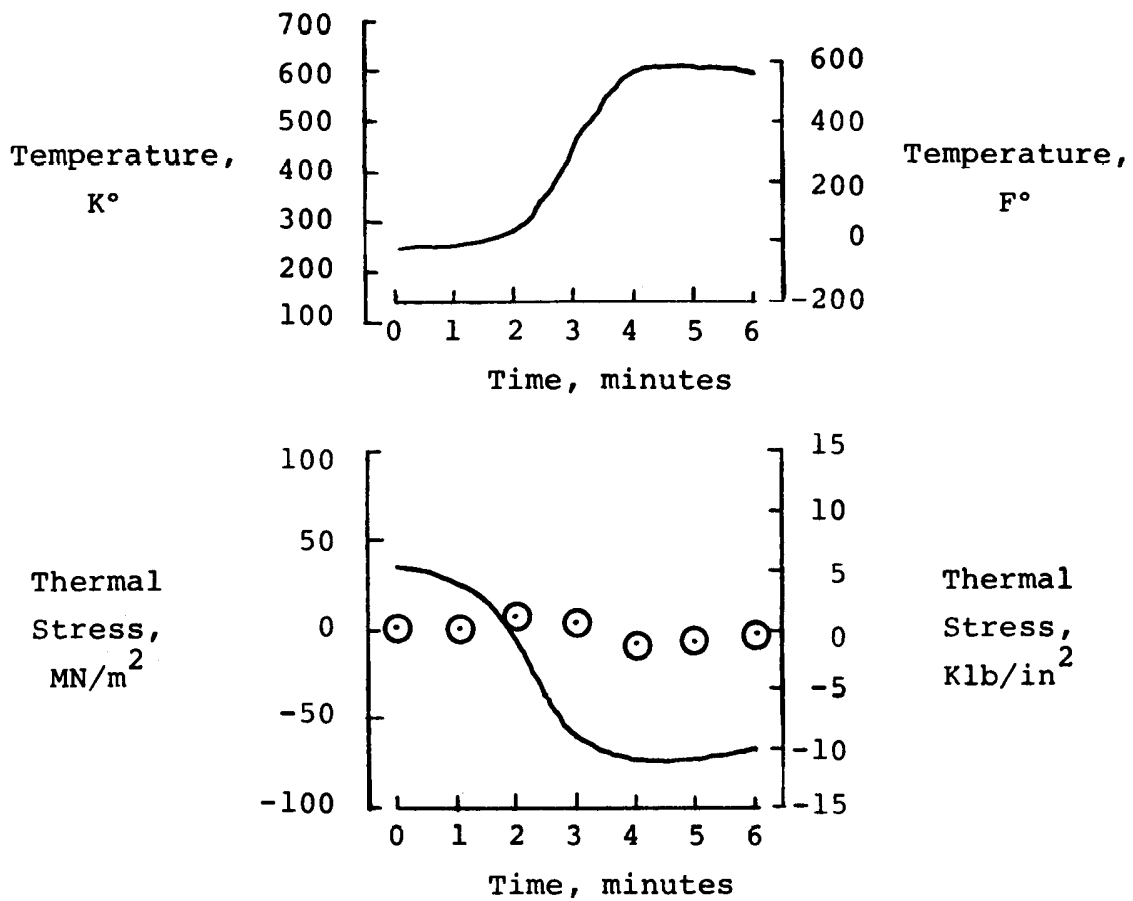
Figure 14. Continued.



(g) Location A.

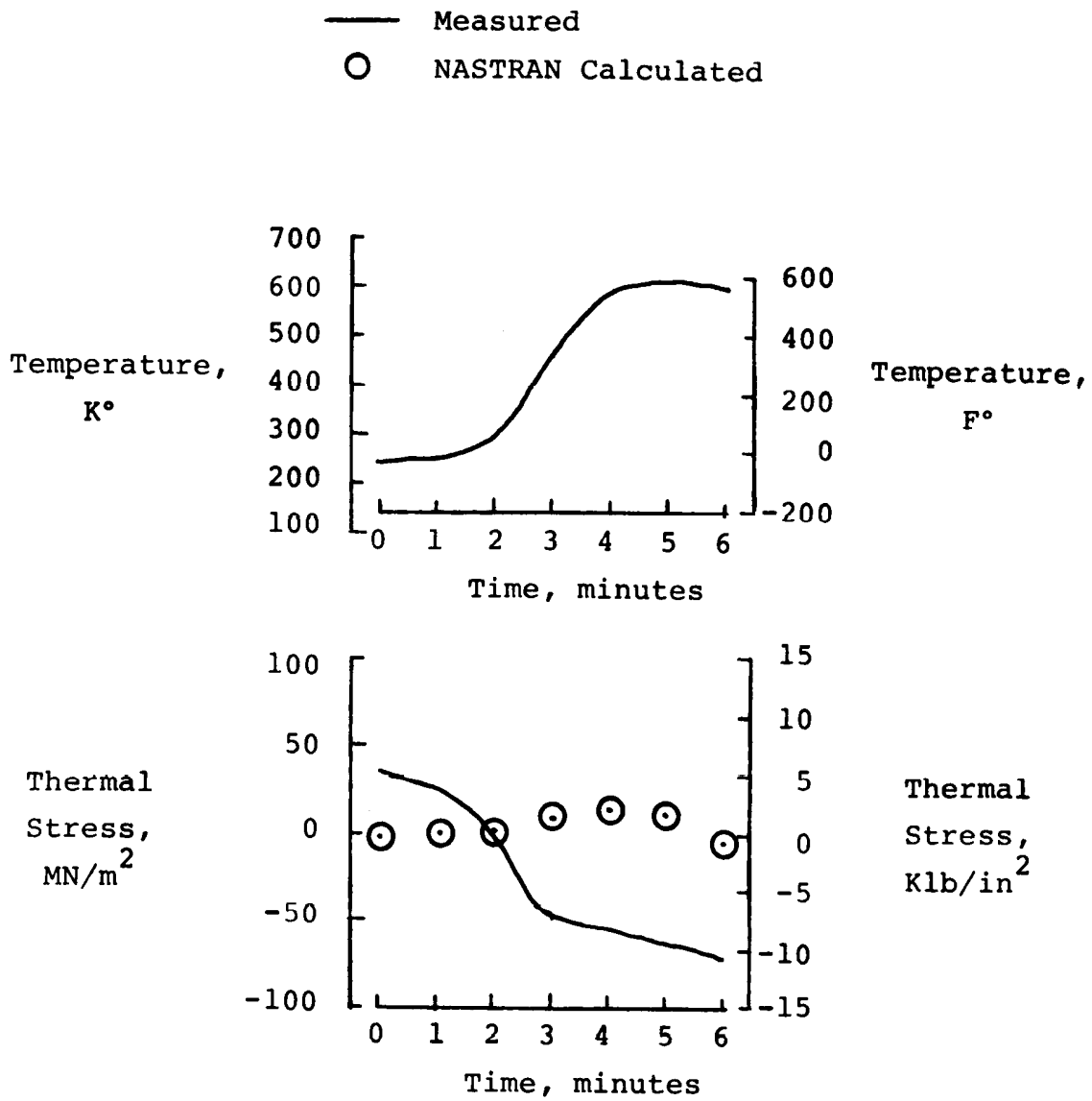
Figure 14. Continued.

— Measured
 ○ NASTRAN Calculated



(h) Location C.

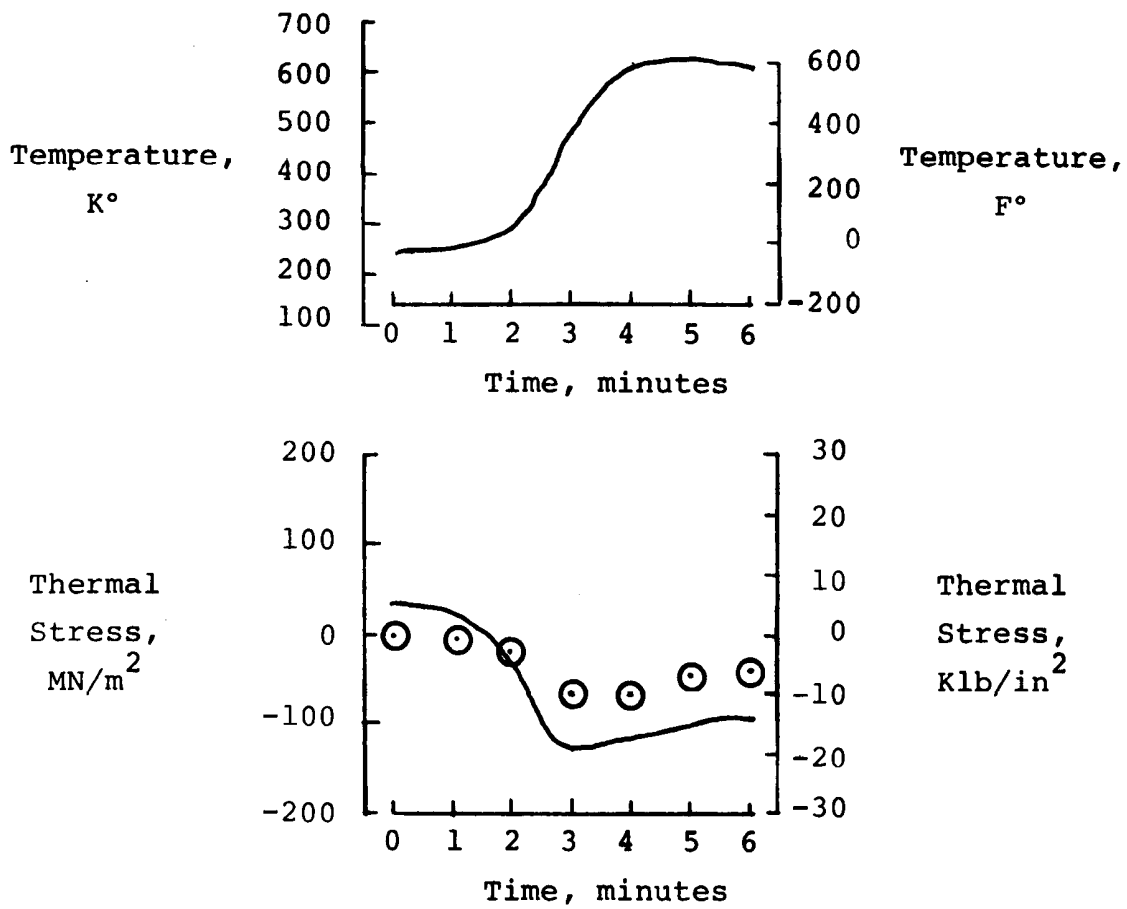
Figure 14. Continued.



(i) Location E.

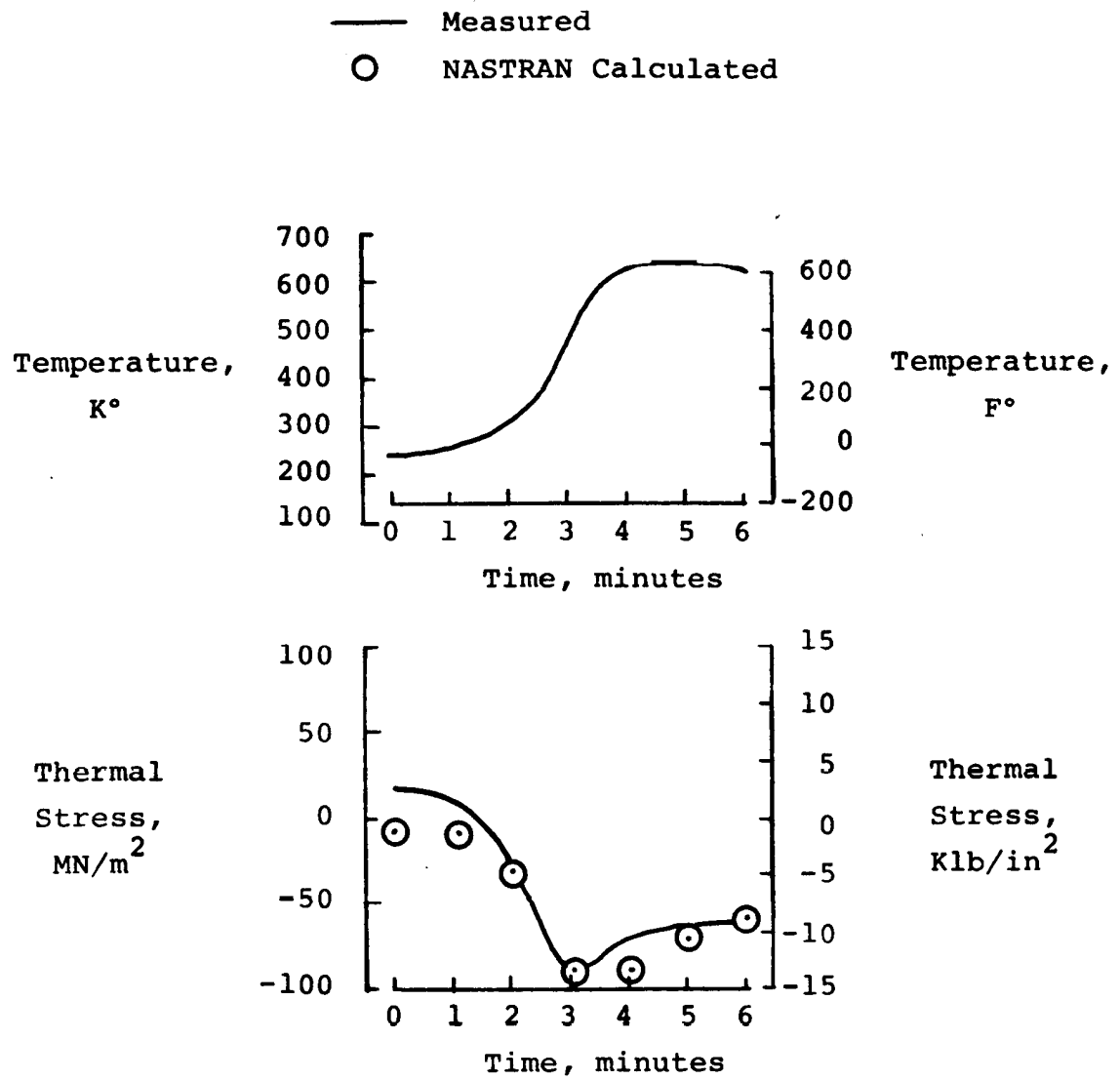
Figure 14. Continued.

— Measured
 ○ NASTRAN Calculated



(j) Location G.

Figure 14. Continued.



(k) Location I.

Figure 14. Concluded.

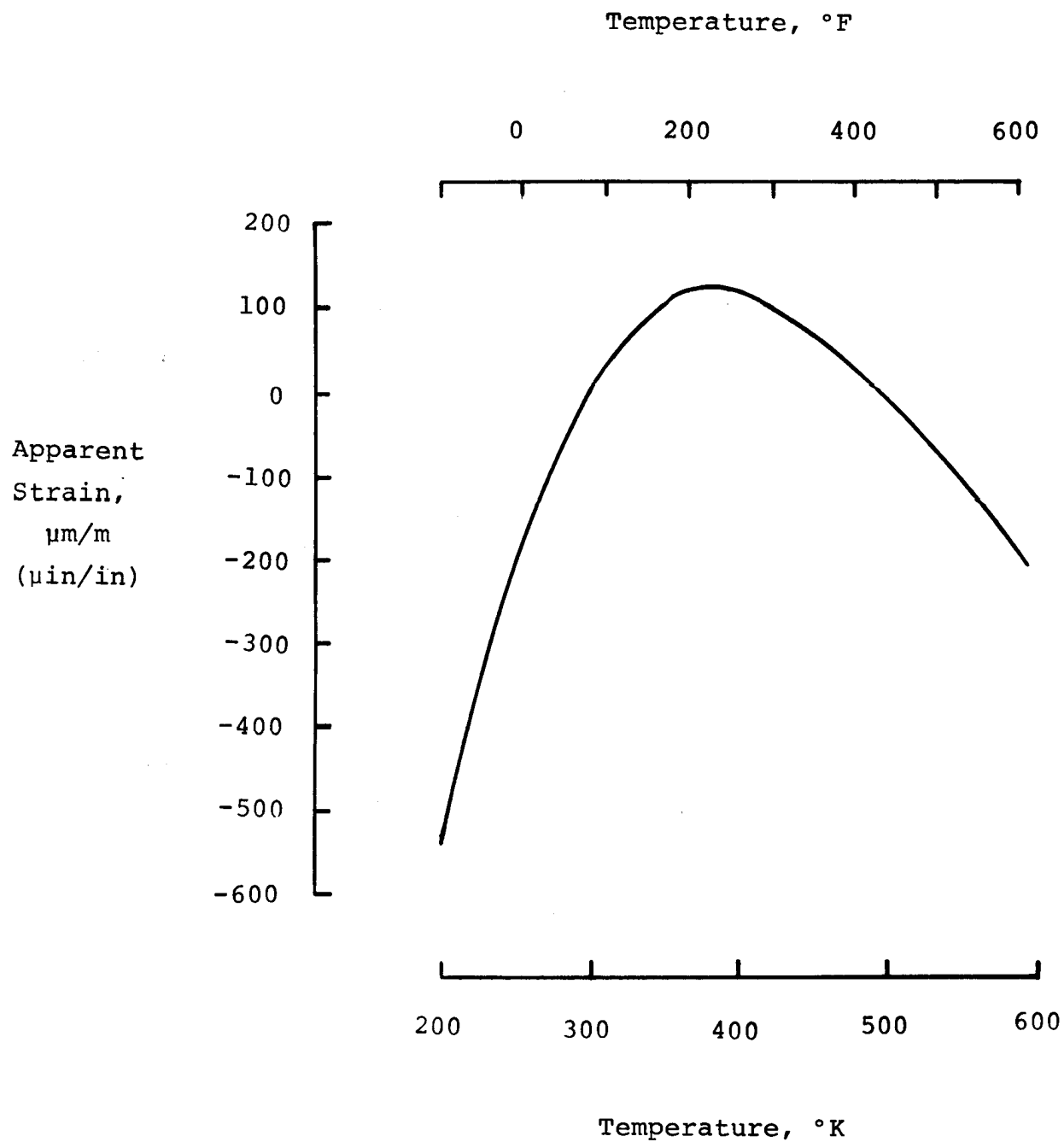
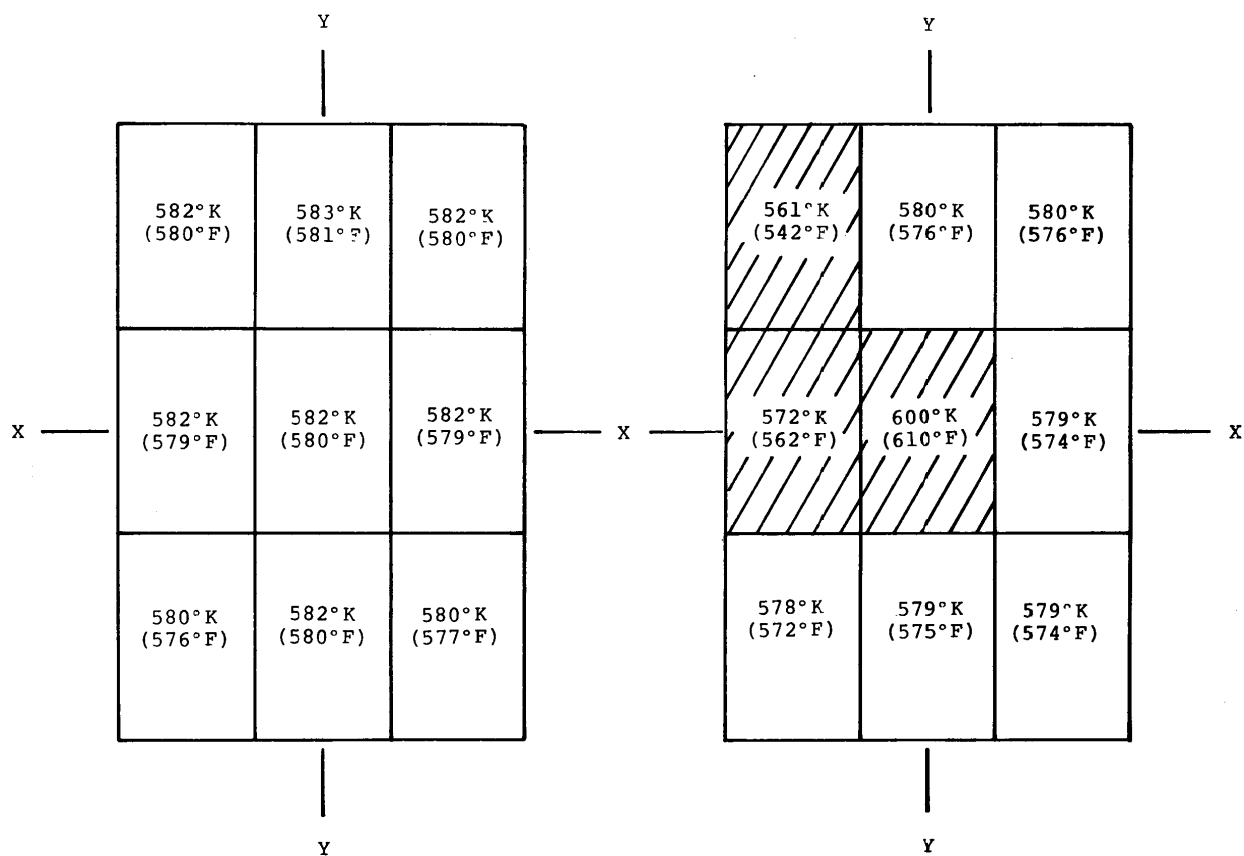


Figure 15. Apparent strain variation with temperature used for the test specimen materials.



(a) Skin temperature distribution of test panel of reference 4.

(b) Skin temperature distribution of current test panel.

Figure 16. Comparison of previous test skin temperature distribution with current test.

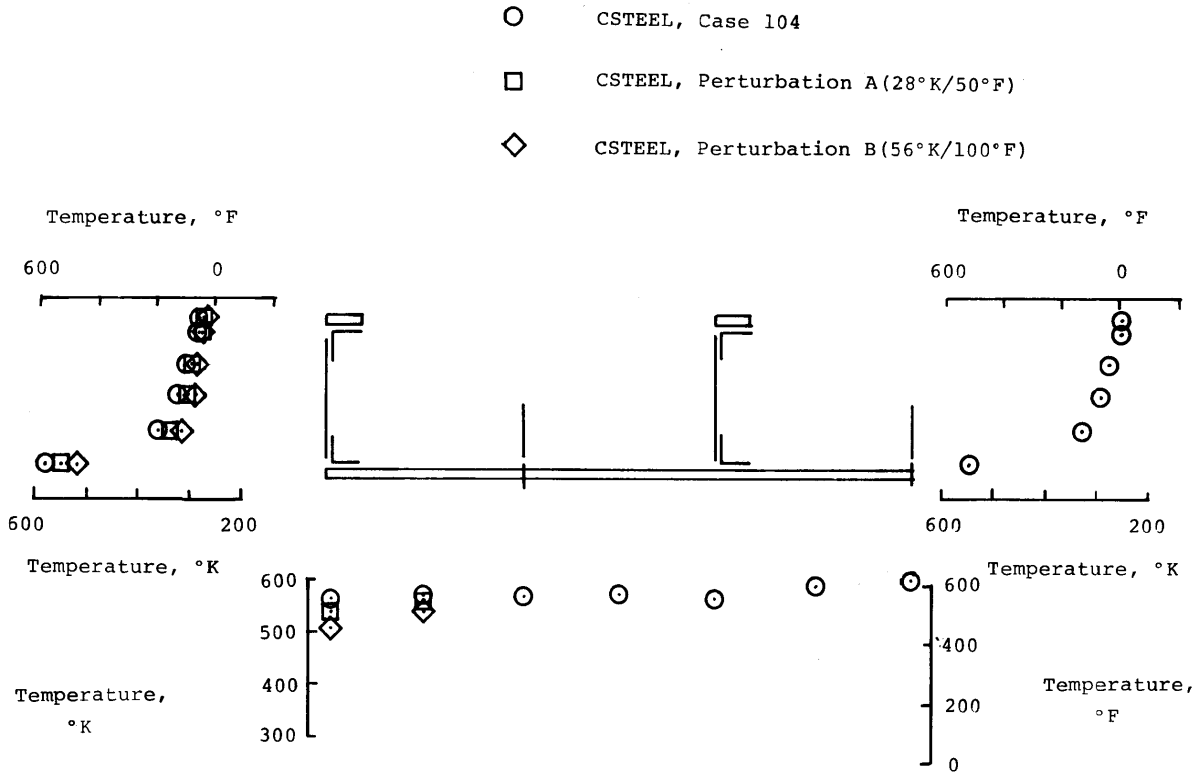


Figure 17. Perturbed temperature distributions used for analysis.

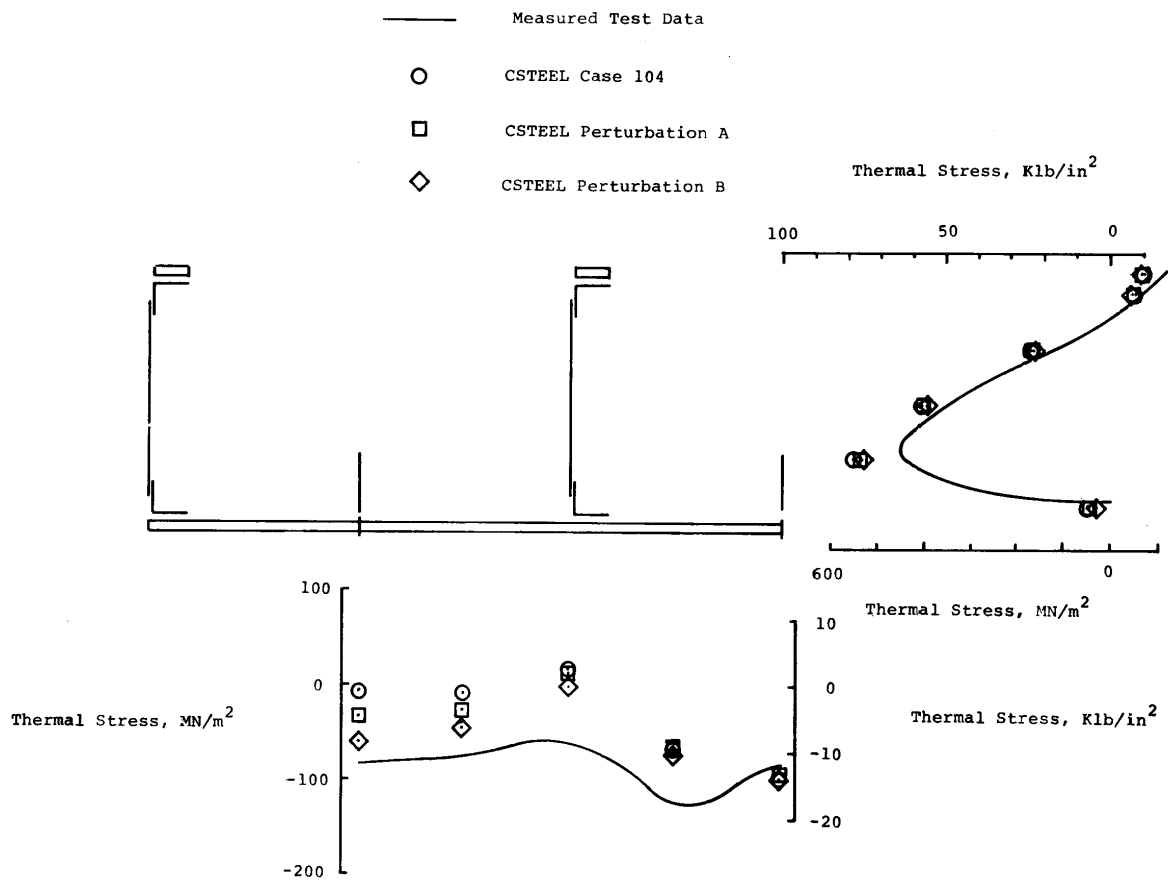


Figure 18. Thermal stress distribution resulting from perturbed temperature distributions.

1. Report No. NASA TM-72862		2. Government Accession No.		3. Recipient's Catalog No.	
4. Title and Subtitle CORRELATION OF PREDICTED AND MEASURED THERMAL STRESSES ON AN ADVANCED AIRCRAFT STRUCTURE WITH SIMILAR MATERIALS				5. Report Date April 1979	
				6. Performing Organization Code	
7. Author(s) Jerald M. Jenkins				8. Performing Organization Report No. H-1086	
9. Performing Organization Name and Address NASA Dryden Flight Research Center P.O. Box 273 Edwards, California 93523				10. Work Unit No. 505-02-24	
				11. Contract or Grant No.	
12. Sponsoring Agency Name and Address National Aeronautics and Space Administration Washington, D.C. 20546				13. Type of Report and Period Covered Technical Memorandum	
				14. Sponsoring Agency Code	
15. Supplementary Notes					
16. Abstract <p>A laboratory heating test simulating hypersonic heating was conducted on a heat-sink type structure to provide basic thermal stress measurements. Six NASTRAN models utilizing various combinations of bar, shear panel, membrane, and plate elements were used to develop calculated thermal stresses. Thermal stresses were also calculated using a beam model.</p> <p>It was found that for a given temperature distribution there was very little variation in NASTRAN calculated thermal stresses when element types were interchanged for a given grid system. Thermal stresses calculated for the beam model compared similarly to the values obtained for the NASTRAN models. Calculated thermal stresses compared generally well to laboratory measured thermal stresses. A discrepancy of significance occurred between the measured and predicted thermal stresses in the skin areas. A minor anomaly in the laboratory skin heating uniformity resulted in inadequate temperature input data for the structural models. The results of this paper indicate a high degree of structural model sensitivity to errors or inadequacies in the temperature information.</p>					
17. Key Words (Suggested by Author(s)) Thermal stresses Hypersonic structures			18. Distribution Statement Unclassified-Unlimited STAR category: 01		
19. Security Classif. (of this report) Unclassified		20. Security Classif. (of this page) Unclassified		21. No. of Pages 41	
				22. Price* \$3.75	

*For sale by the National Technical Information Service, Springfield, Virginia 22161